Geological mapping of Sputnik Planitia on Pluto

Oliver L. White, Jeffrey M. Moore, William B. Mckinnon, John R. Spencer, Alan D. Howard, Paul M. Schenk, Ross A. Beyer, Francis Nimmo, Kelsi N. Singer, Orkan M. Umurhan, et al.

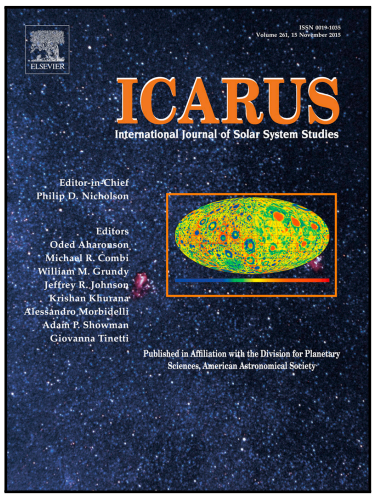

Geological mapping of sputnik planitia on pluto

Oliver L. White , Jeffrey M. Moore , William B. McKinnon , John R. Spencer , Alan D. Howard , Paul M. Schenk , Ross A. Beyer , Francis Nimmo , Kelsi N. Singer , Orkan M. Umurhan , S. Alan Stern , Kimberly Ennico , Cathy B. Olkin , Harold A. Weaver , Leslie A. Young , Andrew F. Cheng , Tanguy Bertrand , Richard P. Binzel , Alissa M. Earle , Will M. Grundy , Tod R. Lauer , Silvia Protopapa , Stuart J. Robbins , Bernard Schmitt , the New Horizons Science Team

PII: S0019-1035(16)30598-X
DOI: 10.1016/j.icarus.2017.01.011
Reference: YICAR 12333

To appear in: *Icarus*

Received date: 2 October 2016
Revised date: 30 November 2016
Accepted date: 6 January 2017

Please cite this article as: Oliver L. White , Jeffrey M. Moore , William B. McKinnon , John R. Spencer , Alan D. Howard , Paul M. Schenk , Ross A. Beyer , Francis Nimmo , Kelsi N. Singer , Orkan M. Umurhan , S. Alan Stern , Kimberly Ennico , Cathy B. Olkin , Harold A. Weaver , Leslie A. Young , Andrew F. Cheng , Tanguy Bertrand , Richard P. Binzel , Alissa M. Earle , Will M. Grundy , Tod R. Lauer , Silvia Protopapa , Stuart J. Robbins , Bernard Schmitt , the New Horizons Science Team, Geological mapping of sputnik planitia on pluto, *Icarus* (2017), doi: 10.1016/j.icarus.2017.01.011

Highlights

- The geology of Sputnik Planitia on Pluto is mapped at 1:2M scale.
- All mapped units are presently being affected by the action of flowing N_2 ice.
- Sputnik Planitia is experiencing convection, glacial flow, and sublimation.
- Condensation of N_2 onto much of Sputnik Planitia creates a bright mantle.
- Blocky H_2O ice mountains and hills have been mobilized by flow of N_2 ice.

GEOLOGICAL MAPPING OF SPUTNIK PLANITIA ON PLUTO

Oliver L. White[1]*, Jeffrey M. Moore[1], William B. McKinnon[2], John R. Spencer[3], Alan D. Howard[4], Paul M. Schenk[5], Ross A. Beyer[6,1], Francis Nimmo[7], Kelsi N. Singer[3], Orkan M. Umurhan[1], S. Alan Stern[3], Kimberly Ennico[1], Cathy B. Olkin[3], Harold A. Weaver[8], Leslie A. Young[3], Andrew F. Cheng[8], Tanguy Bertrand[9], Richard P. Binzel[10], Alissa M. Earle[10], Will M. Grundy[11], Tod R. Lauer[12], Silvia Protopapa[13], Stuart J. Robbins[3], Bernard Schmitt[14], and the New Horizons Science Team.

[1]NASA Ames Research Center, Space Science Division, Moffett Field, CA 94035, USA.
[2]Department of Earth and Planetary Sciences, Washington University, St. Louis, MO 63130, USA.
[3]Southwest Research Institute, Boulder, CO 80302, USA.
[4]Department of Environmental Sciences, University of Virginia, Charlottesville, VA 22904, USA.
[5]Lunar and Planetary Institute, Houston, TX 77058, USA.
[6]The SETI Institute, Mountain View, CA 94043, USA.
[7]University of California, Santa Cruz, CA 95064, USA.
[8]Johns Hopkins University Applied Physics Laboratory, Laurel, MD 20723, USA.
[9]Laboratoire de Météorologie Dynamique, IPSL, Sorbonne Universités, 4 Place Jussieu, 75005 Paris, France.
[10]Massachusetts Institute of Technology, Cambridge, MA 02139, USA.
[11]Lowell Observatory, Flagstaff, AZ 86001, USA.
[12]National Optical Astronomy Observatory, Tucson, AZ 85719, USA.
[13]Department of Astronomy, University of Maryland, College Park, MD 20742, USA.
[14]Université Grenoble Alpes, CNRS, IPAG, F-38000 Grenoble, France.

Manuscript pages: 74
Figures: 15
Tables: 1

Present address of corresponding author: Oliver White, MS 245-3, NASA Ames Research Center, Moffett Field, CA 94035, oliver.l.white@nasa.gov, 281-309-8152 (Cell)

Abstract: The geology and stratigraphy of the feature on Pluto informally named Sputnik Planitia is documented through geologic mapping at 1:2M scale. All units that have been mapped are presently being affected to some degree by the action of flowing N_2 ice. The N_2 ice plains of Sputnik Planitia display no impact craters, and are undergoing constant resurfacing via convection, glacial flow and sublimation. Condensation of atmospheric N_2 onto the surface to form a bright mantle has occurred across broad swathes of Sputnik Planitia, and appears to be partly controlled by Pluto's obliquity cycles. The action of N_2 ice has been instrumental in affecting uplands terrain surrounding Sputnik Planitia, and has played a key role in the disruption of Sputnik Planitia's western margin to form chains of blocky mountain ranges, as well in the extensive erosion by glacial flow of the uplands to the east of Sputnik Planitia.

1. Introduction

Following its flyby of Pluto in July 2015 (Stern et al., 2015), NASA's New Horizons spacecraft has returned high quality images that cover the entire encounter hemisphere of the planet, and which have revealed a highly (and unexpectedly) diverse range of terrains, implying a complex geological history. The centerpiece of the encounter hemisphere is the prominent and informally named Sputnik Planitia, and it is on this feature and its immediate environs that initial geological mapping of Pluto's surface has been focused. This paper presents mapping within an area covered by a mosaic of 12 images obtained by New Horizons' Long-Range Reconnaissance Imager (LORRI) (Cheng et al., 2008) that includes all of Sputnik Planitia and portions of the surrounding terrain (shown in Fig. 1, along with a global context map). In the early stages of analysis of New Horizons images, Sputnik Planitia was recognized to be a highly complex entity that displays a wide range of surface textures and patterns and which is undergoing rapid surface renewal (Stern et al., 2015; Moore et al., 2016; McKinnon et al., 2016). Accordingly, the purpose of this study is to specifically map, describe, and interpret units within the Planitia itself, as well as any units in the surrounding terrain that are considered to be presently directly affected by, or which are directly affecting, Sputnik Planitia, and to determine the sequence of events that formed and modified them. Those terrains within the mapping area that are not directly interacting with Sputnik Planitia at present are generalized as 'Pre-Sputnik Planitia Uplands', and are not examined as part of this mapping study. A nomenclature map of the mapping area is shown in Fig. 2. Note that all feature names used in this paper are presently informal.

1.1 Physiographic setting

The mapped area we present covers just over 2,000,000 km^2, or just over 11% of Pluto's surface area, and measures 2070 km from the northernmost corner (at 69.5°N) to the southernmost corner (at 30.5°S), and 1925 km from the westernmost corner (at 131°E) to the easternmost corner (at 221.5°E). The high

albedo plains of Sputnik Planitia, which have an area of 870,000 km^2 and form the western lobe of the heart-shaped region dubbed Tombaugh Regio, dominate the mapping area. Sputnik Planitia is surrounded by rugged highland terrain: to the west and southeast are the low albedo Cthulhu Regio and Krun Macula respectively; to the east is the high albedo eastern lobe of Tombaugh Regio; to the north is the intermediate albedo Voyager Terra; to the south is the enigmatic feature dubbed Wright Mons, a roughly circular mound ~150 km across with a ~70 km diameter depression at its summit. The terrain to the west and north of Sputnik Planitia are heavily cratered, while those of east Tombaugh Regio are considerably less so; no impact craters have been confirmed in Sputnik Planitia itself in contiguous mapping coverage of 320 m/pixel (Moore et al., 2016) or in any higher resolution strips.

The topography of the mapped area has been derived using stereophotogrammetry (see supplementary online material in Moore et al. (2016) for details of technique) and a digital elevation model (DEM) is shown in Fig. 3. The level of Sputnik Planitia is 3-4 km below the surrounding terrain (Moore et al., 2016), and the plains appear to be virtually flat on a horizontal scale of tens of kilometers. Also apparent in Fig. 3 are the ranges of blocky, chaotically oriented mountains that include (from north to south) al-Idrisi, Zheng-He, Bare, Hillary and Norgay Montes, which skirt the western margin of Sputnik Planitia. The peaks of these mountains reach elevations of up to 5 km above the surrounding plains.

2. Methodology

2.1 Geological mapping

The geologic mapping of Sputnik Planitia reported in this study follows the standard principles of the mapping of extraterrestrial bodies as outlined in Wilhelms (1972, 1990) and Tanaka et al. (2011),. Some of the assumptions of geologic mapping (Wilhelms, 1990) derived solely from images acquired above the study area are that: (1) the scene contains (at least some) landforms that lend themselves to expert

identification; and (2) the landform suites represent the surface manifestations of sequences of deposits separated by discrete boundaries for which the rules of superposition and cross-cutting apply and are hence amenable to being stratigraphically organized. Thus traditional planetary geologic maps are, in reality, geomorphological or physiographic maps being cast, via interpretation, into a geologic map format (Moore & Wilhelms, 2001). The experience of terrestrial field geology strongly indicates that the results of non-ground-truthed, image-based geologic mapping are tentative and, at best, the equivalent of hypotheses. Nevertheless, until ground truth can be acquired, traditional planetary geologic mapping remains at least a very useful mechanism for organizing observations and presenting results (Wilhelms, 1990).

The 12-image LORRI mosaic being used as the mapping base is at a characteristic scale of 386 m/pixel. Mapping is performed at a scale of 1:2M. The entire mapping area has also been covered by Multispectral Visible Imaging Camera (MVIC) imagery with a characteristic scale of 320 m/pixel. Overlying this 320 m/pixel MVIC coverage are three LORRI strips obtained at 234, 117 and 76 m/pixel, as shown in the map in Fig. 4a. We use the 386 m/pixel LORRI mosaic as the mapping base as it offers an optimum combination of resolution and look angle; the look angle of the 320 m/pixel MVIC imagery becomes quite oblique in the northern latitudes of the mapping area. The four additional, higher-resolution observations have not been employed to actually define unit boundaries in our map, but we have referred to them in order help define the finer-scale textures and morphological characteristics of the units, which aids in their interpretation. The difference in resolution between the lowest and highest resolution imagery we have studied is less than a factor of five. Planetary terrains can often appear quite different when viewed in separate imagery that varies in resolution by an order of magnitude or more (e.g. Malin & Edgett, 2000), yet there is no unit that we have mapped that appears very different at 76 m/pixel compared to 386 m/pixel. The 234, 117 and 76 m/pixel LORRI strips cross occurrences of all mapped units, with the exception of the bright, pitted uplands (unit bpu) and the scattered hills (unit sh), for which

the 320 m/pixel MVIC data is the best available. A map of the variation in solar incidence angle across these observations is shown in Fig. 4b.

We define units based primarily on the texture and albedo that they present at the 386 m/pixel scale of the base map used for mapping. We generally use simple, nongenetic labels for mapped units (e.g., the Dark, Ridged Terrain; the Sparsely Pitted Plains). An exception is the Impact Crater unit; impact craters being landforms whose origins we believe can be unambiguously identified. Albedo is the primary distinguishing factor when mapping the contact between the Bright, Cellular Plains and Dark, Cellular Plains, which display similar surface textures at 386 m/pixel. Measured topographic relief is a criterion that is generally not useful for defining units within the map. The stereo topography shown in Fig. 3 is only useful with respect to gauging the reliefs of the mountainous and hilly units in the map (in particular the Chaotic, Angular, Blocky Mountains, the Bright, Pitted Uplands, and the Bright, Chaotic Terrain), as Sputnik Planitia itself is comprised of plains that are virtually flat on a scale of tens of kilometers, and what small-scale topographic relief can be discerned in imagery of the plains (the pitting in particular) is not resolved in the stereo topography. Reliable shape-from-shading DEMs, which achieve a higher resolution than those of the stereo DEMs that is comparable to that of the source image, are not yet available.

New Horizons compositional data revealed by MVIC and the Linear Etalon Imaging Spectral Array (LEISA) (Weaver et al., 2008) have aided in the interpretation of some units within the map, but not actually to define unit boundaries (mainly because the resolution of the data, which is typically at a scale of km/pixel, is too low). Grundy et al. (2016), Protopapa et al. (2017), and Schmitt et al. (2017) have presented maps highlighting surface abundance of H_2O, N_2, CO, and CH_4 across Pluto's encounter hemisphere, and Protopapa et al. (2017) have also shown maps of ice grain size based on Hapke modeling. In the context of our mapping study, this data has been especially useful in assessing the physical state and origins of the Chaotic, Angular, Blocky Mountains (section 4.3.1.) and the Bright,

Pitted Uplands (section 4.4), as well as deducing the cause of the albedo contrast between the Bright, Cellular Plains and the Dark, Cellular Plains (section 4.1.2.).

2.2 Variance mapping

The surfaces of a number of the geological units that have been mapped in Sputnik Planitia display subtle but geologically significant differences in pitted textures both between different units and across single units. Visual inspection of the highest resolution Sputnik Planitia images (at 76 m/pixel) show that there are coherent patterns in the amplitude of the pitting as a function of position within the cells. We have considered various algorithms for providing quantitative, objective, and automated characterization in the amplitude of the pitting, and in the end have found that the local image-intensity variance is highly effective at revealing even subtle spatial variations in the properties of the pits. A variance map shows the variance within a small circular area centered on each pixel in the source image. For each pixel in the image, we measure the intensity variance of the pixels weighted in radial distance from it by a two-dimensional circularly symmetric gaussian kernel to smoothly limit the domain of the variance measurement. The spatial width of the kernel is a compromise between being large enough to encompass a fair sample of pits, while still being small enough to track fine-scale changes within the cells - in practice we use 12-pixels full width at half maximum. With the variance map represented as a gray-scale image, in which smooth areas appear dark and rough areas appear bright, subtle pitting amplitude variations in the source imagery become vividly obvious. Fig. 8 within section 3 demonstrates how this technique is sensitive to the variations in pitted texture.

3. Description of the Geology of Sputnik Planitia

The geological map is shown in Fig. 5. The following sections describe each of the units listed in the map and offer interpretations for their formation and evolution. The exception to this is the “Pre-Sputnik

Planitia Uplands" (unit psu), which are not interpreted to be currently affecting, or being affected by, Sputnik Planitia, and which are therefore beyond the scope of this study. However, we do map impact craters larger than two kilometers in diameter (unit ic) and extensional fractures within the Pre-Sputnik Planitia Uplands, as these features will be mentioned in forthcoming sections. Concise descriptions and interpretations of the 15 units mapped in Fig. 5 (not including the Pre-Sputnik Planitia Uplands) are included in Table 1.

3.1 Cellular plains of Sputnik Planitia

The cellular plains (Fig. 6) occupy the majority of the northern portion of Sputnik Planitia. Here, the plains are divided into ovoid cells reaching several tens of kilometers across and separated by a network of troughs reaching a few kilometers across (shown as black lines in Fig. 5). The troughs commonly display a medial ridge that extends across much of the width of the trough ('2' labels in Fig. 6b) (Moore et al., 2016). While the troughs are resolved to a degree in currently available stereo DEMs (Fig. 3), their vertical relief is comparable to the amplitude of noise within the DEMs (which is especially high in the plains areas in the center of Sputnik Planitia because of the lack of small-scale surface albedo contrast here), so we estimate depths for them of some tens of meters based on their shading at high solar incidence angles. The troughs do not always define the boundaries of cells; in a ~500 km wide region in the center of Sputnik Planitia, the network of troughs becomes less interconnected, and so does not define a system of closely packed cells. 200 cells have been identified within the cellular plains. The median area of a cell is 707.5 km^2 ($\pm\sigma$ of 1441 km^2), with a minimum cell area of 60 km^2 and a maximum of 10,574 km^2. The cumulative size-frequency distribution of the cell areas is shown in Fig. 7. Three types of cellular plains have been identified: the Bright, Cellular Plains (unit bcp), the Dark, Cellular Plains (unit dcp), and the Dark, Trough-Bounding Plains (unit tbp). Where we refer only to "cellular plains" in the text, we are referring to the Bright and Dark, Cellular Plains collectively.

3.1.1 Bright, Cellular Plains

The Bright, Cellular Plains occupy the majority of the southern portion of the cellular plains. This unit displays the highest albedo of the three categories of cellular plains, and the troughs marking the boundaries of the cells are sharply defined here (Figs. 6a and 6b). At the centers of the cells, the surface texture is typically smooth at the 76 m/pixel scale, becoming more densely pitted towards their edges, with pits reaching a few hundred meters in diameter. The resolution of available stereo DEMs (Fig. 3) is too coarse to resolve these pits, but we estimate based on shading that they typically have depths reaching some tens of meters. This contrast in texture between the centers and edges of the cells is highlighted in the variance map in Fig. 8b, which shows that the boundary between the smooth and pitted textures is generally sharply defined and not gradational. The troughs appear dark in the variance map, and instances are encountered where either smooth-textured or pitted zones cut across troughs, or at least mute their relief ('1' labels in Fig. 8b). In small cells seen at the southern end of the image ('2' label in Fig. 8b), compact regions of rough terrain reaching <5 km across exist at the very centers of the cells, giving them a 'bullseye' configuration.

3.1.2 Dark, Cellular Plains

To the north and west of the Bright, Cellular Plains is the Dark, Cellular Plains unit. Cell interiors appear darker than in the Bright, Cellular Plains, but the edges of the cells can still appear bright (Figs. 6c and 6d). The troughs at the cell boundaries can be well defined, as in the Bright, Cellular Plains, but in some instances they appear to fade and dissipate (see '3' labels in the variance map in Fig. 8d). The Dark, Cellular Plains also occur as enclaves reaching tens of kilometers across that are embayed by the Bright, Cellular Plains, most prominently within the interiors of cells proximal to the main contact between the two units (see Fig. 5 and the '3' labels in Fig. 6c). These enclaves become smaller and less numerous with increasing distance to the southeast of the main contact. The main contact itself is characterized by 'filaments' of the Bright, Cellular Plains extend into the Dark, Cellular Plains along the

pathways of troughs ('4' label in Fig. 6c). The variance map in Fig. 8d shows that, as in the Bright, Cellular Plains, the Dark, Cellular Plains exhibit regions of a pitted texture that tend to concentrate at cell boundaries and trough junctions, with smoother regions concentrated in cell centers, although several examples are seen where smooth regions extend all the way to the cell boundaries, and can even form arcuate networks that cross from cell to cell ('4' labels in Fig. 8d).

It should be noted that the variance of the pitted texture in the Dark, Cellular Plains in Fig. 8d appears darker than that for the Bright, Cellular Plains in Fig. 8b. This is not due to the pitted texture in the Dark, Cellular Plains being appreciably smoother than the Bright, Cellular Plains (the scale of their pitted textures in Fig. 8c appears to be similar); nor is it an artifact caused by the lower surface albedo of the Dark, Cellular Plains, as the variance method yields consistent results across an albedo gradient. Instead, it is likely a consequence of the changing illumination across the scene (Fig. 4b), which the variance method is sensitive to. In available imagery, the solar incidence angle for the Dark, Cellular Plains is generally less (~20° to 30°) than that for the Bright, Cellular Plains (~45°-70°), so longer shadows are cast by the pit walls in the Bright, Cellular Plains and the contrast is boosted there as a result, making the pitted texture in the Bright, Cellular Plains seem rougher. For this reason, the variance maps in Figs. 8b and 8d should only be used to compare the respective distributions of pitted and smooth regions within the Bright and Dark, Cellular Plains, and not to assess their absolute surface roughness.

Alcyonia Lacus is a 30 km long by 10 km wide expanse of Dark, Cellular Plains that is surrounded by the Chaotic, Angular, Blocky Mountains (unit abm) and the Chaotic, Inter-Block Material (unit ibm) ('4' label in Fig. 11a). While it is separated by 100 km from the primary expanse of Dark, Cellular Plains in northern Sputnik Planitia, it displays an albedo that is characteristic of that unit, so we have chosen to classify it as Dark, Cellular Plains. It displays faint, dark lineations aligned in a roughly east-west orientation.

3.1.3 Dark, Trough-Bounding Plains

At the northern margin of Sputnik Planitia are the Dark, Trough-Bounding Plains. This unit (with a lower albedo than the Dark, Cellular Plains) congregates around cell boundaries, which here appear as thin, dark lineations reaching ~1 km across (Fig. 6e). Topographic relief at these dark cell boundaries is not readily apparent as it is for boundaries within the Bright, Cellular Plains. In a few rare instances, bright central lineations are resolved within the dark cell boundaries ('6' labels in Fig. 6f). At some locations directly adjacent to the surrounding Pre-Sputnik Planitia Uplands, albedo contrast in the plains reveals lobate flow patterns, and in some cases flow is seen to occur between nunataks (exposed peaks surrounded by glacial ice) of Pre-Sputnik Planitia Uplands material that are protruding above the plains ('5' labels in Fig. 6e) (Stern et al., 2015; Umurhan et al., 2017). The dense surface pitting that is seen within the Dark, Cellular Plains and Bright, Cellular Plains is not generally identifiable within the Dark, Trough-Bounding Plains.

3.2 Non-cellular plains of Sputnik Planitia

Five units are identified in the non-cellular plains of Sputnik Planitia: the Lightly Pitted Plains (unit lpp), the Sparsely Pitted Plains (unit spp), the Deeply Pitted Plains (unit dpp), the Patchy, Pitted, Marginal Plains (unit pmp), and the Dark-Pitted, Marginal Plains (unit dmp). These units are mainly located to the south, east and west of the cellular plains, and display a high albedo comparable to that of the Bright, Cellular Plains. The cellular plains display either a smooth surface texture at 76 m/pixel, or a pitted texture on a scale reaching a few hundred meters, with the pits always displaying an equidimensional planform. The non-cellular plains display a greater variety of surface textures ranging from smooth at 76 m/pixel to coarsely pitted on a scale typically reaching a few kilometers, with the pits displaying a range of planform aspect ratios, from equidimensional to very elongate.

3.2.1 Lightly Pitted Plains

The Lightly Pitted Plains display a surface texture somewhat similar to that of the pitted texture seen within the cellular plains, and feature a shallow, continuous, close-packed pitted texture with pits displaying a fairly consistent diameter of a few hundred meters and having equidimensional planforms (Fig. 9a). The Lightly Pitted Plains mostly occur along the eastern margin of Sputnik Planitia, intermediate between the valley glaciers emptying into Sputnik Planitia and the Bright, Cellular Plains. Occasional enclaves of the Lightly Pitted Plains occur interstitially to mountains and blocks within the Chaotic, Angular, Blocky Mountains (unit abm) and Chaotic, Inter-Block Material (unit ibm) ('3' labels in Fig. 11a).

3.2.2 Sparsely Pitted Plains

The Sparsely Pitted Plains (Fig. 9b) appear mainly smooth and featureless down to 76 m/pixel, but with scattered, isolated pits that typically reach diameters of ~1 km, and which are not as sharply defined as those within the Deeply Pitted Plains (see section 3.2.3). The unit occurs in association with the Lightly Pitted Plains and Deeply Pitted Plains, both in southern Sputnik Planitia and where small patches of the Deeply Pitted Plains are seen at the western and northern margins of Sputnik Planitia.

3.2.3 Deeply Pitted Plains

The Deeply Pitted Plains feature sharply defined pits of varying spatial concentration that show consistently larger diameters than pits in the cellular plains or the Lightly Pitted Plains (Fig. 9c), reaching from a few hundred meters to several kilometers in diameter (Figs. 9c, 9d and 9e). The resolutions of available stereo DEMs are too coarse to resolve these pits, so we cannot infer their depths by this method. However, the Deeply Pitted Plains are the only plains unit where any of the pits are wide enough such that their floors can be resolved in available imagery. The 76 m/pixel imagery is able to resolve shadows within some of the pits (Fig. 9e). We interpret these to be genuine shadows cast across the floors of these pits and not merely the non-illuminated walls of these pits, as the shadows extend across more pixels than

the opposite, illuminated walls (and we assume that the pits are small enough such that their walls are essentially the same height around their circumferences). By performing shadow measurements on the four pits indicated in Fig. 9e, we find that they reach depths between 160 and 190 m, which is more than the tens of meters that we estimate for pits within the cellular plains and the Lightly Pitted Plains. The pits in the Deeply Pitted Plains tend to be relatively widely spaced further north, by distances reaching a few to several kilometers, but they become closely packed further south where the unit borders the Pre-Sputnik Planitia Uplands of Krun Macula. Pits can be single or merge to form doublets, as well as chains that are seen to align parallel to each other (labels '1' to '3' in Fig. 9c). Pit planforms range from equidimensional to elongate; elongate pits and pit chains tend to align N-S. In several instances close to the margin of Sputnik Planitia, dense concentrations of elongated, aligned pits are sometimes seen to form wavelike patterns. The pits in Fig. 9d are amongst the widest in Sputnik Planitia (label '4' marks the widest of all), and in all instances where the floors of pits within the Deeply Pitted Plains are resolved and are not obscured by shadows (e.g. Figs. 9d, 9e, and 9f), the floors always display a low albedo; that marked by label '4' is wide enough such that a rubbly texture can be discerned on its floor. To the south of the Bright, Cellular Plains, chains of joined pits trace the outlines of vaguely triangular polygons, with Sparsely Pitted Plains existing within their centers (Fig. 9f, and marked as 'extinct troughs' in Fig. 5). The Deeply Pitted Plains cover much of the southern portion of Sputnik Planitia, but are also seen to occur as enclaves between cells and along troughs within the Bright, Cellular Plains, and occurrences are seen at the western and northern margins of Sputnik Planitia.

3.2.4 Patchy, Pitted, Marginal Plains

The Patchy, Pitted, Marginal Plains unit occurs along the southeastern, southern and southwestern margins of Sputnik Planitia. It is also seen to occur as enclaves within topographic basins in the Bright, Pitted Uplands of eastern Tombaugh Regio, as well as filling valleys between mountain blocks in Norgay Montes. The unit is characterized by a generally hummocky texture on a scale of a few to several

kilometers, and on a similar scale also typically displays a patchy texture of close-packed pitting (comparable to that seen in parts of the Deeply Pitted Plains), interspersed with smooth, featureless zones (Fig. 9g). In places along the southeastern margin of Sputnik Planitia, the morphology of the unit exhibits characteristics of the Pre-Sputnik Planitia Uplands, including craggy spurs that achieve reliefs of 1 km and extend into the Deeply Pitted Plains to the west ('8' label in Fig. 9h), and what appears to be a very eroded 12 km diameter impact crater ('9' label in Fig. 9h). When viewed at high phase, dark bands reaching a few kilometers across are often seen where the Patchy, Pitted, Marginal Plains occur in valleys leading from the Bright, Pitted Uplands into Sputnik Planitia, the surface of which is a few kilometers lower in elevation ('2' labels in Fig. 13, and mapped as 'valley glacier flow lines' in Fig. 5). The bands are aligned parallel to the valleys. Enclaves of the unit are seen to fill basins and craters within the Pre-Sputnik Planitia Uplands ('7' label in Fig. 9g).

3.2.5 Dark-Pitted, Marginal Plains

The Dark-Pitted, Marginal Plains occur as a NW-SE-aligned strip filling a valley in-between the chaotic mountainous units of western Sputnik Planitia and the Pre-Sputnik Planitia Uplands of Cthulhu Regio, and are somewhat similar in appearance to the Patchy, Pitted, Marginal Plains in that dense pit concentrations alternate with smoother expanses, but the unit does not display the same hummocky relief (Fig. 9i). The Dark-Pitted, Marginal Plains feature equidimensional pits less than a kilometer in diameter ('10' label in Fig. 9i), as well as clusters of closely spaced, low albedo, tendril-like features that reach less than a kilometer across but several kilometers in length, and which commonly align in a roughly N-S orientation. These features show little apparent relief, which may be partly due to the solar incidence angle being low for the Dark-Pitted, Marginal Plains during flyby (typically 40°-50°), combined with the fact that the Dark-Pitted, Marginal Plains are the non-cellular plains unit that is covered by the lowest resolution imagery (234 m/pixel). Small patches of the unit are seen covering crater floors in Cthulhu Regio and Viking Terra (Fig. 10a).

3.3 Mountainous and hilly units of western and eastern Sputnik Planitia

As with the plains units of Sputnik Planitia, no impact craters have been confirmed within any of these mountainous and hilly units in contiguous mapping coverage of 320 m/pixel.

3.3.1 Chaotic, Angular, Blocky Mountains

A discontinuous chain of mountains with apparently random orientations (unit abm, the Chaotic, Angular, Blocky Mountains, see Fig. 11a) extends for hundreds of kilometers along the western boundary of Sputnik Planitia from ~45°N to ~25°S (Moore et al., 2016). Individual blocks can reach tens of kilometers across and elevations of up to 5 km above the surrounding plains, with slopes reaching >30°. Planform aspect ratios of the mountains range from 1:1 to ~4:1. The mountains are mostly close-packed in discrete ranges, although some smaller, isolated blocks are seen towards the interior of Sputnik Planitia, removed by >100 km from the ranges (such as Coleta de Dados Colles, shown by the '2' label in Fig. 11a). The southern boundary of Cthulhu Regio is the only location where isolated mountain blocks are seen surrounded by the Pre-Sputnik Planitia Uplands, rather than by Sputnik Planitia plains units; the mountains here are seen in association with enclaves of the Patchy, Pitted, Marginal Plains unit that fill topographic basins ('3' labels in Fig. 10b). Individual mountain blocks, particularly those in al-Idrisi Montes, tend to display flat or sloping faces with a texture comparable to that seen in the Pre-Sputnik Planitia Uplands that bound Sputnik Planitia to the north; neighboring faces on these blocks sometimes show dark lineations running across them (see inset in Fig. 11a).

3.3.2 Chaotic, Inter-Block Material

The Chaotic, Angular, Blocky Mountains tend to be separated and embayed by the Chaotic, Inter-Block Material (unit ibm, see '1' labels in Fig. 11a), which displays a similarly chaotic texture to the

mountains, but which is at a finer scale, with blocks reaching up to several kilometers across. Perhaps partly due to their smaller sizes, the blocks do not display the complexity that is apparent for blocks within the Chaotic, Angular, Blocky Mountains, and tend to display a high albedo.

3.3.3 Bright, Chaotic Terrain

At the northwestern margin of Sputnik Planitia is the Bright, Chaotic Terrain (unit bct, Fig. 11b), which forms a strip up to 50 km wide between the Pre-Sputnik Planitia Uplands to the north and Chaotic, Inter-Block Material associated with Al-Idrisi Montes to the south. The Bright, Chaotic Terrain features dark massifs and ridges reaching several kilometers across that are separated by bright plains. The unit displays two prominent, east-west-trending, extensional faults (comprising normal faults and graben) that can display up to 1 kilometer of relief ('5' labels in Fig. 11b). The elevation of the Bright, Chaotic Terrain is virtually level with that of the Chaotic, Inter-Block Material that borders it to the south (Fig. 12). Directly to the east of the Bright, Chaotic Terrain is an 80 by 100 km block of the Pre-Sputnik Planitia Uplands that sits on the shoreline of Sputnik Planitia. The block tilts towards the shoreline at an angle of 3° and it is bisected by a graben that is ~500 m deep ('6' label in Fig. 11b), and which is aligned parallel with the fractures seen within the Bright, Chaotic Terrain. Where this graben terminates at the shoreline of Sputnik Planitia, dark flows lines in Sputnik Planitia are seen to converge to a point ('7' label in Fig. 11b).

3.3.4 Dark, Ridged Terrain

Situated at intervals along the margin between the Chaotic, Angular, Blocky Mountains/Chaotic, Inter-Block Material and the Pre-Sputnik Planitia Uplands to their west are elongate strips of the Dark, Ridged Terrain (unit drt). This unit is characterized by low albedo, parallel ridges that can be linear as well as curved, and which display wavelengths from several hundred meters to a few kilometers. The resolution of the stereo DEM in Fig. 3 is too low for these ridges to appear in it. The material forming the

ridges appears to exist on top of a higher albedo substrate, which sometimes appears interstitially to the ridges. The ridges are typically aligned N-S or NW-SE, i.e. roughly parallel to the edge of Sputnik Planitia, but at some locations along the margin between this unit and the Pre-Sputnik Planitia Uplands that border it to the west, the ridges curve such that they align parallel to the border of the unit ('8' label in Fig. 11c).

3.3.5 Scattered Hills

In the eastern portion of central Sputnik Planitia, where it bounds eastern Tombaugh Regio, numerous Scattered Hills reaching a few kilometers in diameter (unit sh) are scattered across the Bright, Cellular Plains and units of the non-cellular plains (Moore et al., 2016). Where they occur within the Bright, Cellular Plains, individual hills as well as clusters of hills are always coincident with the cell boundaries. The hills here tend to collect into densely packed clusters typically reaching several kilometers to a few tens of kilometers across (e.g. Soyuz Colles and Astrid Colles, see '9' labels in Fig. 11d). In the non-cellular plains proximal to the Bright, Pitted Uplands, chains of these hills align along paths of N_2 ice glaciers (see Fig. 13) emanating from the Bright, Pitted Uplands ('10' labels in Fig. 11d). The largest conglomerations of hills are Challenger Colles and Columbia Colles, which form roughly rectangular masses measuring several tens of kilometers across, and which are adjacent to the shoreline of Sputnik Planitia ('11' and '12' labels respectively in Fig. 11e).

3.4 Bright, Pitted Uplands of east Tombaugh Regio

Our mapping area covers a large proportion of the high albedo region of east Tombaugh Regio, much of which has been mapped as Bright, Pitted Uplands (unit bpu, see Fig. 13). This unit has a pervasive pitted texture, with individual pits typically reaching several kilometers across. Pits border each other and are separated by narrow septa. The pits can locally intersect to form distinct NE-SW-trending ridge-and-

trough terrain (Moore et al., 2016). The unit is also marked by chains of especially large pits (reaching up to 10 km across and 1 km deep) that trend NW-SE ('3' labels in Fig. 13, and marked as graben and scarps in Fig. 5), and in which scarp morphologies can sometimes be discerned. The floors of many pits, as well as the floors of wide valleys that separate high-standing expanses of pitted terrain (prominent examples indicated by '1' labels in Fig. 13), have a smooth or pitted texture that we have mapped as the Patchy, Pitted, Marginal Plains (see section 3.2.4). The spatial density of impact craters (unit ic) is low in the Bright, Pitted Uplands (see Fig. S13B in Moore et al. (2016)). A few very degraded, complex craters reach tens of kilometers across, while better-preserved craters with simple, bowl-shaped morphologies reach several kilometers across. Identification of impact craters within the Bright, Pitted Uplands is complicated by the fact that most of the identified impact craters reach diameters that are comparable to those of the pits (typically <20 km), and so discerning pit morphologies from crater morphologies can be challenging.

4. Interpretation of the Geology of Sputnik Planitia

4.1 Cellular plains of Sputnik Planitia

4.1.1 Convection within the cellular plains

The cellular morphology of these plains, the total absence of impact craters in contiguous mapping coverage at 320 m/pixel, and compositional data from the Ralph instrument have led to the hypothesis that Sputnik Planitia consists predominantly of low-viscosity N_2 ice (in a solid solution with far lesser amounts of CO ice) that is in the active process of solid-state convection (Stern et al., 2015; Grundy et al., 2016; Moore et al., 2016; McKinnon et al., 2016; Trowbridge et al., 2016). We interpret the medial ridges that are commonly seen within the troughs ('2' labels in Fig. 6b) to result from the compressive forces that prevail at the cell boundaries, where laterally migrating N_2 ice is converging and pushing up

the ridges at the centers of the troughs. The uniformity of the morphologies of the medial ridges along the lengths of the troughs may be explained by the uniform physical properties of the N_2 ice, which is likely to be kept well mixed by the convection.

The appearances of the Bright, Cellular Plains and Dark, Cellular Plains are similar in that both contain smooth areas that tend to concentrate within the interiors of the cells, while increasingly densely-spaced pitting is seen towards the cell margins (Fig. 8). We interpret the pits to be caused by sublimation of N_2 ice from the surface of the plains into Pluto's atmosphere, but their distribution within the cells can potentially be explained by more than one model for the convective regime within the cellular plains. If the convection forming the cells causes appreciable surface motion of the N_2 ice from the centers of the cells to the edges, as in an isoviscous regime, then the increasing spatial density of the pitted texture may be explained by fresh, upwelling N_2 ice at the centers of the cells undergoing gradual sublimation as it moves laterally outwards towards the cell edges, with the resulting pits being destroyed as the N_2 ice is subducted at the cell edges. However, if a sluggish lid convection regime is prevailing, whereby the surface is in motion, but moves at a much slower rate than the deeper, warmer subsurface (McKinnon et al., 2016), then the variation in pitting across a cell may instead be more representative of the thermal regime of the ice below the surface, rather than of the surface age of the ice. Specifically, heat is conducted through the lid from the subsurface layer, with more heat being conducted at the centers of the cells, which are located above the warmer, upwelling portions of the convective system below. This increased heat flow at the center of the cell would cause annealing of the ice and swift relaxation of any pits that attempt to develop (Moore et al., 2017); the lower heat flow at the cell edges would be insufficient to cause such annealing, and pits that form due to sublimation of the N_2 ice there are preserved (although they would still eventually be destroyed by the subduction of the lid). The compact, rough regions seen at the centers of some cells ('2' label in Fig. 8b) may indicate the focal points of material rising from below, causing disruption of the surface here. Instances where smooth or pitted

regions appear to crosscut troughs dividing cells may indicate instability in the convective system, with cell boundaries decaying as small cells merge to form larger ones.

McKinnon et al. (2016) and Moore et al. (2017) have made independent estimates of the rates of convective flow and sublimation of the N_2 ice respectively, which aid in determining which of these convective regimes applies to Sputnik Planitia. Based on the temperature dependence of N_2 ice viscosity (Yamashita et al., 2010), McKinnon et al. (2016) considered it to be most probable that the N_2 ice layer convects in the sluggish lid regime, and used numerical modeling to estimate average surface horizontal velocities of a few centimeters each terrestrial year for the N_2 ice within the cells, implying a surface renewal timescale of ~500,000 years. The heuristic modeling study of Moore et al. (2017) investigated the respective roles of sublimation and mass wasting in enlarging and infilling pit topography, and found that the pits grow until the timescales of sublimation and mass wasting are comparable. The uncertainties in N_2 ice rheology, and the potential presence of stiffer secondary phases, prohibit a firm estimate for this equilibrium rate at which sublimation within the pits must occur in order to counteract the infilling by mass wasting. Nevertheless, Moore et al. (2017) claimed that it was very likely that the evolution timescale of the pits is rapid, and suggested a value of a few terrestrial years as the timescale over which a 1 km diameter pit might be infilled by creep of ice within a thin layer, assuming that the effective thickness of the layer of N_2 ice is set by the annual thermal skin depth, which is ~30 meters for N_2 ice. In contrast, viscous relaxation of a 1 km diameter pit within a homogeneous N_2 ice layer several kilometers thick could take as little as a terrestrial day, which is an unrealistic timescale for pit evolution. Despite the intrinsic uncertainties, the results of these studies indicate that convective flow of the N_2 ice takes place on a much longer timescale than the formation (and maintenance of the relief) of pits by sublimation. We consider a sluggish lid regime to be the more likely mode of convection within Sputnik Planitia. Such a lid would be more likely to have the necessary rheology to support the observed pit relief enough to maintain equilibrium between mass wasting and sublimation, as compared to an isoviscous

regime, in which case the consistent viscosity profile throughout the kilometers-thick N_2 ice layer would lead to rapid infilling of the pits as suggested by the modeling of Moore et al. (2017).

We also interpret the rapid onset of dense pitting towards the edges of cells (Figs. 8b and 8d) to be more consistent with a sluggish lid regime. Modeling of convection within Sputnik Planitia by Umurhan et al. (2016) indicates a steep lateral gradient in heat flow to the surface between zones of warm, upwelling N_2 ice at cell centers and cooler, downwelling N_2 ice at cell margins. The distinctly segregated smooth and pitted portions of the cells are respective manifestations of these different thermal conditions that prevail underneath the lid, with conduction of heat through the lid controlling where on the surface pit morphologies are stable (i.e. high heat flow causing annealing of pit morphologies in the center and low heat flow allowing stable pit morphologies at the edges, as discussed earlier). In an isoviscous regime, a smoother gradient in the increase in the spatial density of pitting would be expected, as pit growth would be more a function of the age of the N_2 ice at the surface rather than the thermal conditions at depth, and so steadily larger pits would be seen from the centers to the edges of cells as the laterally flowing and ageing N_2 ice progressively sublimates. In addition, the radially outwards flow of the surface N_2 ice in an isoviscous regime (which would attain a higher rate than for sluggish lid convection) would be expected to cause increasing distortion and elongation of pit planforms towards the cell boundaries, which is not observed. Instead, the consistently circular planforms of pits across the surfaces of the cells implies a slow rate of lateral motion of the surface N_2 ice that is consistent with sluggish lid convection.

The region in the center of Sputnik Planitia, where the network of troughs within the Bright, Cellular Plains becomes less interconnected, and does not define a system of closely packed cells, may be explained by the N_2 ice being thicker here. It has been hypothesized that the ices of Sputnik Planitia are occupying an ancient impact basin (Schenk et al., 2015; Nimmo et al., 2016), and since the surface of Sputnik Planitia is essentially level (Fig. 3), the thickness of the ice would be expected to increase towards the center of the Planitia. Not only would larger convection cells be expected for thicker ice, but with a greater vertical distance for the convecting ice to travel, the influence of factors interfering with the

convective motion may be enhanced relative to where it is thin. In particular, the Rayleigh number for thicker ice will be larger than for thinner ice, such that the convection pattern changes from being static to time varying. The increasing thickness therefore causes the network to reorganize at a faster rate, thereby preventing formation of well-defined cells reaching a few tens of kilometers across that are bordered by troughs.

4.1.2 Cause of albedo variation across the cellular plains

Possible causes of the low albedo of the Dark, Cellular Plains include entrainment of dark material within the ice or deposition of it as a surficial layer; a higher surface roughness for the Dark, Cellular Plains relative to the Bright, Cellular Plains on a scale of tens of meters; and/or a larger ice grain size in the Dark, Cellular Plains relative to the Bright, Cellular Plains. An explanation must also account for the observation that the network of troughs extends across both units: differences between the two units evidently do not affect the process of convection that occurs across all the cellular plains. At the 76 m/pixel scale of the highest resolution images of the Bright and Dark, Cellular Plains, the two units display a comparable surface texture of pitting on a scale up to a few hundred meters, alternating with regions that appear smooth at the available image resolution (Fig. 8). We consider it unlikely that a contrast in surface roughness at an unresolved scale is responsible for their different albedos, as the solar incidence angle for the Bright, Cellular Plains is typically higher (~45°-70°) than it is for the Dark, Cellular Plains (~30°-45°) (Fig. 4b), meaning that the Dark, Cellular Plains would have to be extremely rough compared to the Bright, Cellular Plains in order to explain the observed albedo contrast. Confident assessment of whether surface roughness is a factor would require multi-angular observations (particularly at high phase angles) that are not available given the limited coverage of New Horizons. Regarding ice grain size, the optical paths through larger ice grains will be longer, and it will therefore be more likely that a photon traversing such a path gets absorbed (assuming a non-zero absorption coefficient) (Hapke, 1993). The albedo of coarser-grained ice should therefore be lower than that of

finer-grained ice. The path length map in Fig. 5B of the Hapke modeling study of Protopapa et al. (2017) shows that the N_2 ice of the Bright, Cellular Plains in fact shows a larger grain size (typically $>5 \times 10^5$ μm) than the Dark, Cellular Plains (typically $<5 \times 10^5$ μm).

In order to resolve this apparent paradox, we consider data from MVIC and LEISA that show N_2, CO and CH_4 absorption across all of Sputnik Planitia (Grundy et al., 2016). Arguments developed in Moore et al. (2016) concerning isostasy in Sputnik Planitia imply that CH_4 forms a surficial layer across the plains, and does not represent a major constituent of Sputnik Planitia itself, which is predominantly N_2, with smaller amounts of CO. This argument is supported by the Hapke modeling of Protopapa et al. (2017), which found that a CH_4 concentration of only ~0.3% within Sputnik Planitia is most consistent with New Horizons spectral observations. The weak N_2 and CO absorptions are stronger within an area corresponding closely to the Bright, Cellular Plains, compared to those within the Dark, Cellular Plains (see Fig. 1 in Grundy et al. (2016), Fig. 5 in Protopapa et al. (2017), and Figs. 15 and 24 in Schmitt et al. (2017)). Based on this observation, we consider it likely that the low albedo of the Dark, Cellular Plains is caused by the presence of a dark component, which acts to reduce the N_2 and CO absorption seen across these plains, and which would also offset any brightening effect caused by the ice here having a smaller grain size than in the Bright, Cellular Plains. The presence of this material may in fact be the reason why the ice grains are smaller in the Dark, Cellular Plains than in the Bright, Cellular Plains, as it can pin grain boundaries and prevent grain growth within the compact polycrystalline structure of the ice (Barr and McKinnon, 2007). The identity of such a material is likely to be tholins, a complex mixture of carbonaceous macromolecules that are prevalent across Pluto's surface, and which continuously deposit onto the surface from a tholin haze formed within the atmosphere (Gladstone et al., 2016; Grundy et al., 2016). If the N_2 ice of the Dark, Cellular Plains has been undergoing prolonged convection, as well as sublimation at its surface, then continuous entrainment of tholins, in conjunction with reduction of the volume of the N_2 ice mass via sublimation (if no introduction of fresh N_2 ice is recharging it), would cause the concentration of the non-volatile tholins within the ice to increase. Sublimation of the surface ice may

also cause the residual tholins to build up as a layer of lag on the surface in a manner comparable to how the lag in Callisto's dark, inter-crater plains is interpreted to form (e.g. Moore et al., 1999; White et al., 2016).

The configuration of the contact between the Bright and Dark, Cellular Plains (whereby the former embays outcrops of the latter in cell interiors and also intrudes into the latter along the paths of troughs) causes us to hypothesize that a thin mantle of bright, pure N_2 ice is covering the cellular plains here, and is thick enough to obscure the lower albedo of the darker N_2 ice beneath it, but not thick enough to mask or soften the topographic relief of the troughs, ridges and pits when viewed at 76 m/pixel resolution. We speculate that the mantle may reach as much several meters thick. Significantly, the Bright, Cellular Plains form part of a continuous high albedo zone that stretches into eastern Tombaugh Regio (see Fig. 5 in Buratti et al., 2017). We interpret N_2 ice to have condensed onto and coated the Bright, Pitted Uplands of eastern Tombaugh Regio (see section 4.4) as well as the plains of eastern Sputnik Planitia. As we have noted previously, the Bright and Dark, Cellular Plains both display pitting on a scale of less than a few hundred meters, indicating that sublimation of N_2 ice is taking place to some extent across all of the cellular plains. However, the absence of a bright N_2 ice mantle in the Dark, Cellular Plains indicates that this area represents a zone of net sublimation of N_2 ice from Sputnik Planitia, which causes the dark, tholin-enriched, convecting ice mass to be exposed at the surface. In contrast, the Bright, Cellular Plains and eastern Tombaugh Regio represent a zone of net condensation of N_2 ice. Changing insolation with latitude is certainly one factor that influences the geographical distribution of preferential sublimation and condensation: the northern extent of the bright terrain in both the plains and the Bright, Pitted Uplands is ~30°N, which is the present Arctic Circle and so the southernmost latitude that can experience continuous insolation over a diurnal period at least once during an orbit. An apparent consequence of this is that plains north of 30°N currently represent a zone of preferential N_2 ice sublimation. This behavior is consistent with the results of climate modeling (Bertrand & Forget, 2016; Forget et al., 2017), and the boundaries of the cellular plains that are bright will therefore change with Pluto's obliquity (which is

currently 120°, but varies between 103° and 127° on a 2.8 million terrestrial year cycle (Van Hemelrijck, 1982; Dobrovolskis and Harris, 1983; Dobrovolskis et al., 1997; Earle and Binzel, 2015; Binzel et al., 2017)). However, the band of Dark, Cellular Plains extending south of 30°N down the western margin of Sputnik Planitia (Fig. 5) indicates that factors besides latitude also affect N_2 sublimation and condensation. This region of Sputnik Planitia is proximal to the Chaotic, Angular, Blocky Mountains, which can display topographic relief reaching multiple kilometers, and we speculate that they may influence local atmospheric circulation in a way (possibly through katabatic winds) that prevents net condensation of N_2 ice here. The albedo contrast between the Dark and Bright, Cellular Plains may actually be enhanced by continued sublimation/condensation via a feedback mechanism: if the Dark, Cellular Plains are never recharged with pure N_2 ice, then prolonged sublimation from the surface will cause the plains to darken even further as the concentration of tholins in the ice increases. This would increase heat absorption in the Dark, Cellular Plains and enhance sublimation of N_2 ice, more of which will therefore become available for condensation on the Bright, Cellular Plains, the brightness of which would cause them to be colder, and therefore less susceptible to sublimation, than the Dark, Cellular Plains.

The transition from the Dark, Cellular Plains to the Bright, Cellular Plains coincides with the northeastern boundary of the region of disconnected troughs within central Sputnik Planitia, and we interpret the configuration of the contact between the two to be governed by variations in heat flow in the shallow subsurface stemming from the transient convective systems within the dark N_2 ice here. These variations in heat flow would determine where on the surface sublimation or condensation preferentially occurs. The presence of enclaves of Dark, Cellular Plains surrounded by Bright, Cellular Plains within the interiors of cells (Fig. 5 and '3' labels in Fig. 6c) is interpreted to indicate the presence of transient upwelling of warm N_2 ice from within Sputnik Planitia, which as well as annealing any surface pits, also prevents condensation of N_2 ice onto the surface in quantities that would obscure the dark N_2 ice underneath. Away from these enclaves of Dark, Cellular Plains, where colder ice is descending, the lower

heat flow will instead promote condensation of N_2 ice onto the surface, and so these areas are covered by the bright N_2 ice mantle, including the 'filaments' of Bright, Cellular Plains that appear to intrude along the paths of troughs that bound cells in the Dark, Cellular Plains (Fig. 5 and '4' label in Fig. 6c). We do note that the existence of pits within the bright mantle at the edges of cells indicates that sublimation of N_2 ice is also occurring here. This may seem paradoxical, but we suggest that the sublimation and condensation that produce the pitting and bright mantle respectively may be operating at different timescales, with convection and climate as respective controlling factors. We consider it to be the case that the mantle is covering the pits, and that the pits are not forming within the mantle, as such pits are also seen to form in the Dark, Cellular Plains where no mantle is interpreted to exist. Moore et al. (2017) estimate that the competing processes of sublimation and mass wasting that influence pit morphology are occurring on a timescale on the order of multiple terrestrial years. Condensation of N_2 ice onto the surface must therefore be occurring on a timescale faster than this in order to maintain a continuous mantle across the pitted surface. The thinness of the mantle is demonstrated by the fact that we estimate maximum reliefs of some tens of meters for these pits, and yet their morphologies are not appreciably masked or softened by the mantle when viewed at 76 m/pixel resolution. Once continuous coverage of the mantle has been established, a net balance between sublimation and condensation likely exists, with condensation being strongest during the winter, and sublimation being strongest in the summer; if there were no sublimation of the mantle to check its growth, then it would be much thicker than the several meters that we estimate for it. In this sense, the bright mantle is subject to climatic cycles at both the obliquity and seasonal timescales, its large-scale areal coverage being defined primarily by Pluto's obliquity cycles (as evidenced by its northern boundary coinciding with Pluto's present Arctic Circle), while its thickness would fluctuate on an annual cycle. The patches of Dark, Cellular Plains become smaller and sparser in an eastwards direction away from the contact, implying that climatic conditions evolve such that condensation of N_2 ice becomes more widespread across the plains, eventually allowing it to cover the entire surface of individual cells, including the centers as well as the margins. Figure 14 is

a graphic that illustrates our model for how sublimation and condensation of N_2 ice varies across Sputnik Planitia and eastern Tombaugh Regio and how it is governed by ephemeral convection in the center of the Planitia, at the contact between the Bright and Dark, Cellular Plains.

4.1.3 Alcyonia Lacus

The absence of pits within Alcyonia Lacus ('4' label in Fig. 11a), its smooth boundary with surrounding units, and its faintly lineated texture set it apart from the expanses of Lightly Pitted Plains that also occur interstitially to the mountain blocks of al-Idrisi Montes ('3' labels in Fig. 11a), and imply a distinct origin for this isolated expanse of the Dark, Cellular Plains. The absence of pits indicates that Alcyonia Lacus is currently being resurfaced in some way, and/or that its rheology is unable to support pit topography. The relatively smooth boundaries of the Lacus, whereby the Chaotic, Angular, Blocky Mountains and Chaotic, Inter-Block Material do not intrude into its interior, indicate that this may not be a passive feature, but is actively defining its own boundaries. These observations suggest that Alcyonia Lacus is an active glacial feature, in which flow of the N_2 ice is sufficient to close pits that form through sublimation, as well as to define a smooth margin for the Lacus by shepherding inter-block material to its edges. The dark lineations may also be manifestations of flow within the Lacus. The Lacus may be located above a 'hot spot' away from the main body of Sputnik Planitia that is mobilizing N_2 ice and causing any blocky material within the zone of mobilization to drift to its edges. Alternatively, Stern et al. (2017) hypothesize that this feature may once have been a 'pond' of liquid N_2, the stability of which was maintained during a past era of especially high atmospheric pressure (120-150 millibars), and which has since frozen.

4.1.4 Dark, Trough-Bounding Plains

The very low albedo Dark, Trough-Bounding Plains are interpreted to be where an especially high concentration of tholins is entrained within the ice. The albedo is certainly too low to be explained by

surface roughness or ice grain size. The dark, narrow boundaries of the cells most probably originated in the same fashion as cell boundaries elsewhere in the cellular plains, i.e. as convergence zones of convecting N_2 ice. The thin, bright, medial lineations that are occasionally seen within the dark cell boundaries ('6' labels in Fig. 6f) may represent the same trough/ridge structure seen elsewhere in the cellular plains, but which is clogged by tholins, obscuring the topographic relief of the trough. However, the generally simpler structure of the cell boundaries within the Dark, Trough-Bounding Plains may indicate that convective activity in this marginal region of Sputnik Planitia is less vigorous than in deeper portions occupied by the Dark and Bright, Cellular Plains, causing removal of the dynamic support of cell boundary topography. The presence of an expanse of Deeply Pitted Plains here (at 46.5°N, 172°E) may be another manifestation of the reduced capacity for convection to be sustained here. If the Dark, Trough-Bounding Plains do feature an especially high concentration of tholins, it is likely too high to be explained solely by concentration via prolonged entrainment as well as volatile depletion via sublimation as is interpreted to occur in the Dark, Cellular Plains; some other process must preferentially concentrate them at these locations. Convective motion in the ice may cause them to be concentrated at the edges of cells, and because the Dark, Trough-Bounding Plains are adjacent to the shoreline of Sputnik Planitia, where there are no mountain ranges separating them from the Pre-Sputnik Planitia Uplands and where the N_2 ice is expected to be shallower than towards the center of the cellular plains, tholins embedded in the H_2O ice crust underneath Sputnik Planitia may be getting dredged up and assimilated by convective motion and concentrated within the shallow N_2 ice here. The portions of the Dark, Trough-Bounding Plains that display lobate flow morphologies at the boundary with the surrounding Pre-Sputnik Planitia Uplands, where the cellular structure is absent ('5' labels in Fig. 6e), indicate that the N_2 ice is undergoing lateral flow here (Umurhan et al., 2017). Because no pits are observed within these lobate flows, the rate of flow is presumably sufficient to completely relax the morphologies of any sublimation pits before they reach diameters that can be resolved in available imagery.

4.2 Non-cellular plains of Sputnik Planitia

The region of Sputnik Planitia that contains the non-cellular plains is located far to the south of the present Arctic Circle and currently experiences a regular diurnal cycle and high solar incidence angles (>50°). Climate modeling by Bertrand & Forget (2016) and Forget et al. (2017) has shown that a consequence of these insolation conditions is that the southern portions of Sputnik Planitia presently experience strong condensation of N_2 ice, hence we interpret the high albedo of the plains here to indicate the presence of a thin mantle of N_2 ice, with a low concentration of tholins, like that which covers the Bright, Cellular Plains. As with the cellular plains, this pure N_2 ice layer presumably covers a more substantial body of older, darker N_2 ice that forms the bulk of the non-cellular plains, and advances and retreats as insolation conditions change with Pluto's obliquity cycles.

4.2.1 Lightly Pitted Plains

The Lightly Pitted Plains (Fig. 9a) exhibit a pitted texture that is comparable to that seen at the edges of cells within the cellular plains, and like those pits, these are interpreted to result from superficial sublimation of N_2 ice from the surface of Sputnik Planitia, with the pits only reaching a few hundred meters in diameter. The occurrence of the Lightly Pitted Plains in a broad, discontinuous swath separating the Bright, Cellular Plains from the valley glaciers within the Patchy, Pitted, Marginal Plains along the eastern margin of Sputnik Planitia, and from the Deeply Pitted Plains to the south (Fig. 5), indicates that the Lightly Pitted Plains may represent comparatively fresh N_2 ice introduced via the valley glaciers to Sputnik Planitia. Sublimation is evidently taking place at the surface of these plains, but based on how we interpret the Deeply Pitted Plains to form, they do not exist within regions of Sputnik Planitia where the flow conditions are conducive to shearing of the ice and associated sublimation that enlarges the pits to the sizes encountered in the Deeply Pitted Plains. The small expanses of Lightly Pitted Plains that occur interstitially to mountain blocks ('3' labels in Fig. 11a) are interpreted to be passive features

that exist merely where there is an absence of the Chaotic, Inter-Block Material filling the spaces between large mountains.

4.2.2 Sparsely Pitted Plains

The Sparsely Pitted Plains (Fig. 9b), which tend to be intimately associated with both the Lightly Pitted Plains and the Deeply Pitted Plains, display scattered, shallow pits that present subdued and apparently smoothened relief, and which tend to reach a kilometer in diameter (comparable in scale to pits seen in the Deeply Pitted Plains). If it is natural for N_2 ice in Sputnik Planitia to eventually develop a pitted texture via sublimation if left unperturbed (like that of the Lightly Pitted Plains), then the Sparsely Pitted Plains may therefore be experiencing resurfacing that is eliminating pitted textures on this kilometer scale. The pits with softened relief may be undergoing infill by creep of the low-viscosity N_2 ice, and also mantling by condensation of N_2 ice from the atmosphere. For pits with dark floors in the Deeply Pitted Plains, the low albedo of the floor is evidently sufficient to heat and promote rapid sublimation of any N_2 ice that condenses onto it, ensuring that the floor remains uncovered.

4.2.3 Deeply Pitted Plains

We have observed that the floors of individual pits of the Deeply Pitted Plains unit always display a low albedo when they are large enough such that their floors can be resolved (Figs. 9d, 9e, and 9f). One hypothesis to explain the low albedo is that it is caused by the presence of dark material covering the floors, specifically the tholins that are entrained within the ice underneath the bright surficial layer of N_2 ice. As sublimation of the N_2 ice progresses and pits deepen, the entrained tholins are liberated and build up on the floors of the pits as a lag deposit. The low albedo of the tholins would initially enhance heating, and therefore promote further sublimation and pit growth rates, in the N_2 ice that underlies them, but eventual accumulation of a certain thickness of tholins on their floors would presumably act to suppress further sublimation (e.g. Moore et al., 1999; White et al., 2016). In a similar fashion, instigation of

shallow crevasse formation via shearing of the N_2 ice within the open plains of southern Sputnik Planitia (Moore et al., 2017) could lead to enhanced sublimation and pit formation via the same process of tholin liberation and subsequent entrapment on the floors of the pits. Given the low viscosity of N_2 ice, the rate of pit growth via enhanced sublimation would have to compete with the rate of pit infilling via creep of the ice, a process which Moore et al. (2017) have shown can take place on a timescale as short as a few terrestrial years. An alternate hypothesis for the low albedo floors is that sublimation of the N_2 ice has penetrated all the way through the N_2 ice layer, revealing a dark substrate underneath Sputnik Planitia. This scenario is not especially likely for where the Deeply Pitted Plains exist between cells of the Bright, Cellular Plains ('1' label in Fig. 6a), as the N_2 ice in this roughly circular northern lobe of Sputnik Planitia is thought to be filling a deep impact basin reaching many kilometers deep (Schenk et al., 2016; Nimmo et al., 2016), and our shadow measurements (Fig. 9e) indicate that these pits are likely not more than 200 m deep. The scenario is more plausible for Deeply Pitted Plains in southern Sputnik Planitia, where the N_2 ice is interpreted to be shallower than that in northern Sputnik Planitia, although a confident estimate of its thickness here has not yet been made.

The Deeply Pitted Plains display some characteristics that we interpret to indicate the southwards flow of N_2 ice in southern Sputnik Planitia. One of these is that individual pits are frequently elongated in a roughly N-S orientation, and tend to combine to form long pit chains that are also oriented roughly N-S; such pit chains are especially well-formed in central southern Sputnik Planitia (Figs. 9c and 9d). Clusters of these elongated pits can display curved, wavelike patterns that seem to indicate a flow field (Moore et al., 2017). If so, then the orientations of elongated pits across Sputnik Planitia may be governed by structural anisotropy within the ice that is related to flow direction. As noted above, shearing of the N_2 ice parallel to its southwards flow direction in southern Sputnik Planitia may initiate crevasse formation in the plains that are then widened and deepened by sublimation, creating the elongate, N-S oriented pits. Given the low latitude at which these pits are situated, the N-S elongation may be enhanced by high incidence insolation of these pits, whereby more energy is received on the north- or south-facing walls

(depending on the season), causing preferential sublimation here compared to the east- and west-facing walls. The dark, pitted lineations that trace quasi-polygonal outlines to the south of the Bright, Cellular Plains (Fig. 9f) may also represent another manifestation of the general southwards flow of ice. These polygons are interpreted to be former cells that previously experienced convection within the cellular plains of Sputnik Planitia. Southwards motion of the ice would have shifted these cells away from the convective zone, ceasing the rapid resurfacing that stemmed from the convection, and causing their relief to relax. Several active cells at the southern extreme of the Bright, Cellular Plains display dark tholins filling their bounding troughs, and the dark boundaries of the polygonal outlines may therefore represent 'extinct' troughs where the trough relief has relaxed away, leaving the tholin deposits to mark the outline of the former cell. The polygons appear elongate in a N-S orientation, and the same southwards motion of the ice may have stretched the 'extinct' troughs along this dimension. With no convectional resurfacing of the N_2 ice taking place here, sublimation of the ice along the 'extinct' troughs would be promoted by heating resulting from the low surface albedo of the tholins, accounting for the occurrence of Deeply Pitted Plains along the boundaries of the 'extinct' troughs ('5' label in Fig. 9f).

4.2.4 Patchy, Pitted, Marginal Plains

The hummocky relief of the Patchy, Pitted, Marginal Plains, and its occasional adoption of high-relief morphological characteristics that N_2 ice alone could not support, and which are akin to those of the Pre-Sputnik Planitia Uplands that border it (Figs. 9g and 9h), indicates that these plains represent a N_2 ice layer covering expanses of Pre-Sputnik Planitia Uplands, with the N_2 ice dampening the relief of the underlying topography. The sharply segregated distribution of densely pitted and featureless zones is likely a manifestation of differential physical properties throughout the layer, and may be related to variations in N_2 ice thickness as well as flow state. The Patchy, Pitted, Marginal Plains have been mapped in several places across the study area, and while its texture is always considered to represent shallow N_2 ice covering underlying topography, its genesis may vary between different locations. Where the unit

covers the floors of pits and valleys in the Bright, Pitted Uplands (section 4.4), it likely represents N_2 ice that has condensed onto the Bright, Pitted Uplands, and flowed down into the basins (Howard et al., 2017). Where the Bright, Pitted Uplands border Sputnik Planitia, the unit is seen to form valley glaciers flowing into Sputnik Planitia. The dark marginal bands that characterize these glaciers merge where smaller glaciers feed into larger ones (Moore et al., 2016; Howard et al., 2017), in a manner similar to lateral moraines merging to form medial moraines on terrestrial glaciers (see '2' labels in Fig. 13). The fact that the bands are only faintly visible at low phase, but are sharply defined at high phase, indicates that they are caused by a rough surface texture rather than a difference in albedo between the material that forms them and the flowing N_2 ice underneath. The bands most likely represent material eroded from the surrounding Bright, Pitted Uplands that has been deposited on the flowing ice, and which is forming rubbly lateral moraines along the margins of the valley glaciers (Howard et al., 2017). These glacial systems are almost certainly currently active. The occurrence of the Patchy, Pitted, Marginal Plains in valleys between the high-elevation mountain blocks of Norgay Montes in the southwest of Sputnik Planitia (Fig. 5, the only instance where this unit is intimately associated with the Chaotic, Angular, Blocky Mountains) perhaps indicates that condensation of sublimated N_2 ice is taking place here as it is in the Bright, Pitted Uplands, although formation of valley glaciers does not seem to have occurred here.

The Patchy, Pitted, Marginal Plains that line the southeastern and southern margins of Sputnik Planitia do not appear to be flowing down from the dark Pre-Sputnik Planitia Uplands of Krun Macula, in which there appears to be no source of N_2 ice as there is in the Bright, Pitted Uplands. Instead, the Patchy, Pitted, Marginal Plains are seen to overlie and embay the Pre-Sputnik Planitia Uplands material (lower right quadrant in Fig. 9g), which implies that the southwards motion of N_2 ice in southern Sputnik Planitia has caused it to override low-lying portions of the Pre-Sputnik Planitia Uplands here. Climatic cycles that are tied to Pluto's obliquity cycles (Stern et al., 2017) will cause the N_2 ice plains to alternately advance and recede. When maximum obliquity is reached during a 2.8 Myr obliquity cycle, atmospheric pressure is at a maximum, and the condensation temperature of N_2 is achieved across a maximum area of

the surface (Bertrand and Forget, 2016). This causes N_2 ice to be stable across a broader area of the Pre-Sputnik Planitia Uplands than it is at present. Pluto's last obliquity extreme (of 103°) was 840,000 terrestrial years ago, and N_2 ice has been receding from this high stand since then, meaning that these isolated patches of N_2 ice plains are interpreted to represent residual enclaves of the Patchy, Pitted, Marginal Plains left behind within topographic basins of the Pre-Sputnik Planitia Uplands ('7' label in Fig. 9g) after recession of the front.

4.2.5 Dark-Pitted, Marginal Plains

The Dark-Pitted, Marginal Plains (Fig. 9i) appear to share characteristics of the Deeply Pitted Plains and the Patchy, Pitted, Marginal Plains. The isolated setting of these plains suggests that they are not affected by the large-scale mobilization of N_2 ice that is occurring across the rest of Sputnik Planitia. The Dark-Pitted, Marginal Plains appear to be covering relatively flat expanses in the Pre-Sputnik Planitia Uplands, and seem to be experiencing recession in places. This is especially evident where an isolated patch of it is seen to fill a rimless impact crater 13 km across within a valley in Viking Terra (Fig. 10a), indicating that the Dark-Pitted, Marginal Plains were once more expansive across the floor of this valley. As with the Patchy, Pitted, Marginal Plains on the southeastern margin of Sputnik Planitia, the Dark-Pitted, Marginal Plains are also interpreted to have been undergoing retreat from a glacial maximum during the last period of extreme obliquity 840,000 terrestrial years ago. The presence of sub-kilometer, equidimensional pits ('10' label in Fig. 9i) like those seen in other Sputnik Planitia plains units indicates that sublimation of N_2 ice from these plains is taking place. The fact that any relief of the dark, tendril-like features ('11' label in Fig. 9i) is difficult to discern calls into question their status as pits, but given that their widths are on a similar sub-kilometer scale to the equidimensional pits that they are associated with, and that their organization into aligned clusters is similar to the arrangement of better-resolved pits seen in the Deeply Pitted Plains (compare Fig. 9i with Figs. 9c and 9d), we consider it highly probable that these features are indeed elongate pits. The Dark-Pitted, Marginal Plains border the Pre-Sputnik

Planitia Uplands of Cthulhu Regio, and also embay a 80 by 50 km nunatak of Cthulhu Regio that emerges from the plains at 0°N, 164.5°E. This close association between the Dark-Pitted, Marginal Plains and Cthulhu Regio suggests that the Dark-Pitted, Marginal Plains overlie much of this eastern boundary of Cthulhu Regio. This may explain why so many of the pits display a low albedo, in that the ice of the Dark-Pitted, Marginal Plains may be thin enough such that the pits are as deep as the ice is thick, and are exposing dark terrain of Cthulhu Regio that underlies the ice (a scenario that we have mentioned may also apply to some of the pits of the Deeply Pitted Plains in southern Sputnik Planitia). The NE-SW-aligned, elongate planforms of many of the pits, and their clustering to form wavelike patterns, indicates that flow of ice associated with recession from the Pre-Sputnik Planitia Uplands may be occurring from the contact between the plains and Cthulhu Regio to lower elevations where the Dark-Pitted, Marginal Plains border the Chaotic, Inter-Block Material and Chaotic, Angular, Blocky Mountains of Sputnik Planitia.

We note that there are other instances of 'outliers' of N_2 ice plain units ponding within depressions in the Pre-Sputnik Planitia Uplands to the west and north of Sputnik Planitia, with each interpreted to mark the past advance of N_2 ice plains across the surface during periods of high obliquity. They include Patchy, Pitted, Marginal Plains filling valleys within southern Cthulhu Regio (Fig. 10b), and a tentative identification of Dark, Trough-Bounding Plains filling an 18 km diameter impact crater within Voyager Terra (Fig. 10c). In the present era, the N_2 ice is relatively shielded from direct solar illumination on the floors of valleys and impact craters, and so is less susceptible to sublimation.

4.3 Mountainous and hilly units of western and eastern Sputnik Planitia

4.3.1 Chaotic, Angular, Blocky Mountains and Chaotic, Inter-Block Material

The great relief and steep slopes of the Chaotic, Angular, Blocky Mountains (Fig. 11a) indicate that they are composed of a more rigid material than the N_2 ice in which they are situated (Stern et al., 2015; Moore et al., 2016), and it has been confirmed through spectroscopy that they are formed from H_2O ice

(Grundy et al., 2016), which is extremely strong and inert at Pluto's surface thermal conditions. H_2O ice is also seen in the Pre-Sputnik Planitia Uplands to the west of the mountains, and has been hypothesized to be the main crust-forming material on Pluto (e.g. McKinnon et al., 1997; Hussmann et al., 2006). Moore et al. (2016) interpreted the blocks to be fragments of preexisting ice crust that have been detached from the surrounding Pre-Sputnik Planitia Uplands, and subsequently rotated and transported, by the low-viscosity N_2 ice of Sputnik Planitia, which is denser than the H_2O ice, and which would efficiently exploit weaknesses in the H_2O ice crust. H_2O ice has a density of 0.935 g cm^{-3} between 40 and 100 K (Petrenko and Whitworth, 1999), while N_2 ice has a density of 0.942 to 1 g cm^{-3} between 36 and 63.15 K (Scott, 1976). Consideration of isostasy within Sputnik Planitia (Moore et al., 2016) implies that the keels of many of the larger blocks at the edges of Sputnik Planitia are likely grounded on the shallow base of the Planitia here, but smaller blocks that exist further to the interior of Sputnik Planitia (such as Coleta de Dados Colles, '2' label in Fig. 11a), where the N_2 ice thickness is interpreted to be higher, may actually be mobile and 'floating' within the N_2 ice. The alternating dark and bright lineations that mark the surfaces of some mountain blocks (inset in Fig. 11a) resemble layering seen in the walls of craters in the Pre-Sputnik Planitia Uplands (Moore et al., 2016). Such layering may be indicative of climate cycles in Pluto's early history (Stern et al., 2017), and which is now exposed not only in these crater walls, but also in the sides of mountain blocks that have since broken off from the Pre-Sputnik Planitia Uplands (Binzel et al., 2017). We consider the Chaotic, Inter-Block Material ('1' labels in Fig. 11a) to have a similar genesis to the Chaotic, Angular, Blocky Mountains, but the finer texture may indicate breaking up of the mountain blocks into smaller fragments and/or size filtering thereafter if the blocks are mobile in the N_2 ice.

The mobility of the mountain blocks within the N_2 ice may serve to explain why some blocks are seen to be resting on the surface of the Pre-Sputnik Planitia Uplands of southeast Cthulhu Regio (Fig. 10b). These mountains are associated with ponded N_2 ice that fills basins within this terrain. As described in section 4.2.5, we interpret these N_2 ice patches to have been emplaced during periods of high obliquity

and glacial advance, when Sputnik Planitia was more expansive across this terrain, and now exist as remnants of the former N_2 ice coverage left behind during the current period of glacial recession. The mountains that are perched on the Pre-Sputnik Planitia Uplands here would have been embayed by the N_2 ice plains during the past high stand of Sputnik Planitia, and being mobile within the plains, they would have been transported to their present locations and been left stranded during glacial retreat.

4.3.2 Bright, Chaotic Terrain

The appearance of the Bright, Chaotic Terrain (Fig. 11b), with multi-kilometer sized dark massifs separated by bright plains, is somewhat intermediate between those of the Pre-Sputnik Planitia Uplands to the north and the Chaotic, Inter-Block Material of Sputnik Planitia to the south. Spectral imaging indicates that the Bright, Chaotic Terrain displays an abundance of N_2 ice (Fig. 1 in Grundy et al., 2016; Fig. 15 in Schmitt et al., 2017), and we surmise that this unit represents a portion of Pre-Sputnik Planitia Uplands in which topographic lows have been covered with N_2 ice. The Bright, Chaotic Terrain is amongst the lowest elevation terrain seen anywhere on Pluto, and this in itself may be cause for condensation of N_2 onto the surface here due to the decreasing temperature with decreasing altitude that characterizes Pluto's lower atmosphere (Gladstone et al., 2016). However, we note the existence of deep impact craters located within Cthulhu Regio directly to the west of Sputnik Planitia that are within the permanent diurnal zone of Pluto's surface (i.e. these craters currently receive less insolation than the Bright, Chaotic Terrain which is presently in Pluto's Arctic) and which attain lower elevations than the Bright, Chaotic Terrain, yet some display N_2 ice coverage on their floors while others do not (Fig. 5). As such, we surmise that there must be an additional factor besides the low elevation that concentrates N_2 ice within the Bright, Chaotic Terrain, and we consider the presence of regional-scale extensional tectonism, in the form of the east-west-trending normal fault scarps and graben within the Bright, Chaotic Terrain and the tilted block to its east ('5' and '6' labels in Fig. 11b), to be significant in this respect. As noted in Howard et al. (2017), the convergence of dark flow lines in Sputnik Planitia towards the point where the

graben of the tilted block intersects the shoreline ('7' label in Fig. 11b) raises the possibility that the low-viscosity N_2 ice is exploiting this structural weakness in the crust and is draining into the subsurface to form a conduit network. Its capacity for intrusion into the subsurface along fault planes would be enhanced by the fact that N_2 ice is denser than the H_2O ice crust. The elevation of the Bright, Chaotic Terrain decreases towards the shoreline of Sputnik Planitia; a consequence of this is that much of it is roughly level with and even slightly lower in elevation than the Chaotic, Inter-Block Material to the south (Fig. 12). It is therefore plausible that the N_2 ice that covers low-lying terrain within the unit has been emplaced via overflow directly from Sputnik Planitia. N_2 ice may also potentially emerge onto the surface along fault planes from a subsurface network that is itself sourced from drainage from Sputnik Planitia. Due to its higher density than H_2O ice, N_2 ice would not naturally rise along these planes, so subsidence of the surface is likely to be instrumental in exposing pockets of N_2 ice. However, if the overburden pressure that the N_2 ice is subjected to is sufficiently high to cause pressure melting, which would cause it to become less dense than the surrounding H_2O ice (0.807 g cm^{-3} and 0.935 g cm^{-3} respectively), then ascent of liquid N_2 and its subsequent refreezing upon reaching the surface would be plausible. We therefore interpret the Bright, Chaotic Terrain to be Pre-Sputnik Planitia Uplands that are in an advanced stage of disruption, fragmentation and subsidence resulting from regional-scale extensional tectonism that is being exploited by intrusion of mobile N_2 ice from Sputnik Planitia. The tilted block of rough plateau material is also experiencing extensional tectonism and subsidence, but the forces acting upon it have evidently not yet begun to fragment it. This interpretation would imply that the tilted block and Bright, Chaotic Terrain represent progressive stages in the break-up of the Pre-Sputnik Planitia Uplands to eventually transform to the Chaotic, Angular, Blocky Mountains and Chaotic, Inter-Block Material that line the margin of Sputnik Planitia. The disruption and fragmentation of Pre-Sputnik Planitia Uplands around Sputnik Planitia may therefore still be an active phenomenon due to the abundant evidence that the N_2 ice of Sputnik Planitia itself is currently mobile.

4.3.3 Dark, Ridged Terrain

The ridges of the Dark, Ridged Terrain (Fig. 11c) appear to be superseding a bright substrate that has a blocky texture on a scale comparable to that of the Chaotic, Inter-Block Material. Howard et al. (2017) tentatively interpret the ridges to be recessional moraines of tholin-rich materials deposited on top of the Chaotic, Inter-Block Material during retreat of glaciers formerly covering the region, although acknowledged that this interpretation may be contradicted by the apparently young age of the mountainous units in Sputnik Planitia relative to glacially carved landscapes in the Pre-Sputnik Planitia Uplands. A perplexing aspect of the unit is its highly discrete coverage – it has been mapped in three locations along the western margin of Sputnik Planitia, and at each location the boundary of the dark material with surrounding units is sharply defined. The predominant orientation of the ridges parallel to the edge of Sputnik Planitia may support the glacial moraine hypothesis, but if the ridges are moraines, then there is the question of why their deposition is confined only to these discrete expanses of the inter-block material, unless deposition was originally more widespread and moraines elsewhere have been removed through some means. The origin of the dark material and the reasons for its distribution are uncertain, but we suggest an alternative hypothesis whereby the ridged texture may originate from compressive forces exerted on the inter-block material by westward momentum of the mountains brought on by convection in the cellular plains. Such a mechanism is perhaps better disposed than the recessional moraine hypothesis to explain the instances where the ridges curve to become parallel to the boundary of the unit. A compressional hypothesis for the origin of the ridges would also be more consistent with the apparently young age of this unit relative to the heavily cratered glacial landscapes in the Pre-Sputnik Planitia Uplands, as it would allow both the dark material and the inter-block material to have experienced recent modification, rather than the dark material representing an ancient deposit sitting on top of the younger inter-block material.

4.3.4 Scattered Hills

Moore et al. (2016) and Howard et al. (2017) suggested that the Scattered Hills (Fig. 11d) formed through erosion of the 'bedrock material' in the Bright, Pitted Uplands by glacial flow of N_2 ice, causing chunks reaching a few kilometers in size to break off and then 'float' in the denser N_2 ice as they are rafted into the interior of Sputnik Planitia by the glaciers. This would explain why the hills align in chains that are coincident with the paths of glaciers. Upon entering the cellular plains, the convective motions of the N_2 ice would cause the floating hills to be pushed to the edges of the cells, where they congregate into densely packed groups. The same convective motions may also shepherd the hills along cell boundaries and further into the interior of Sputnik Planitia – the most isolated hill is more than 300 km from the eastern shoreline of Sputnik Planitia. Challenger and Columbia Colles (Fig. 11e) are the largest accumulations of these eroded fragments, and we interpret them to be grounded on the shallow base of Sputnik Planitia, in a similar fashion to how we interpret the larger mountains along the western margin of Sputnik Planitia to be grounded. While the resolution of LEISA data is low compared to the sizes of these hill clusters, spectral imaging of Challenger and Columbia Colles (Fig. 30 in Schmitt et al., 2017) indicates a moderate abundance of H_2O ice that is comparable to that of the Bright, Pitted Uplands, supporting the hypothesis that these hills are derived from that unit, and are buoyant within the N_2 ice plains.

4.4 Bright, Pitted Uplands

The low impact crater spatial density of the Bright, Pitted Uplands implies a younger age for them relative to the Pre-Sputnik Planitia Uplands in general, which is consistent with their mantled and heavily modified appearance: the R-plot for the "east Tombaugh" region in Fig. S13B of Moore et al. (2016) indicates an age not exceeding ~2 Gyrs, while the R-plot for Pre-Sputnik Planitia Uplands within the "northern latitudes" (i.e. to the north of the northern boundary of Sputnik Planitia) indicates an age for them that is slightly younger than the Late Heavy Bombardment (LHB) vicinity of 4 Gyr. As with the bright N_2 ice plains in central and southern Sputnik Planitia, we interpret the high albedo of the Bright,

Pitted Uplands to be caused by recent condensation of N_2 ice onto this terrain as a thin coating. Flow downslope of the low-viscosity N_2 ice that coats the pit walls (estimated to reach slopes of up to 30° (Moore et al., 2016)) causes it to pool on pit floors and in valleys, where it forms the Patchy, Pitted, Marginal Plains unit ('1' labels in Fig. 13) (Howard et al., 2017; Umurhan et al., 2017). This continuous mobilization of N_2 ice allows efficient destruction of impact craters, although there are a handful of craters >10 km in diameter that are sufficiently large (and perhaps also young) such that their morphologies are somewhat preserved.

Exactly what concentrates N_2 ice specifically in this eastern region of Tombaugh Regio is uncertain. Howard et al. (2017) suggested a glacial cycle whereby N_2 ice that is sublimated from Sputnik Planitia is transported to east Tombaugh Regio by atmospheric circulation, condenses onto the landscape, and then returns to Sputnik Planitia via glacial flow. Climate modeling performed by Forget et al. (2017) indicates that wind velocities larger than several meters per second can result from the condensation and sublimation of N_2, whereby inward flows form during the night when N_2 condenses, and outward flows occur when N_2 sublimates in the afternoon. However, these flows occur on all sides of Sputnik Planitia, not just the east side, and so we speculate that the surface of east Tombaugh Regio may have some unknown property that causes it to be an efficient sink for N_2 condensation.

The origin of the pitted texture of the Bright, Pitted Uplands is also ambiguous, but is likely related to the composition of the material that underlies the N_2 ice mantle. Howard et al. (2017) noted that while the Bright, Pitted Uplands are nearly uniformly bright, spectral imaging indicates that N_2 ice is concentrated in the plains occupying the valleys and pit floors, while the pit crests themselves are richer in CH_4 ice (Grundy et al., 2016). While it is beyond the limits of our mapping area, to the east of the Bright, Pitted Uplands there exists what has been referred to as the 'bladed terrain' (see Fig. 3B in Moore et al., 2016). This terrain displays a strong CH_4 signature (Grundy et al., 2016), it has a pit/crest texture that appears reminiscent of that of the Bright, Pitted Uplands, but which is not mantled by N_2 ice and which displays a more aligned fabric. The boundary between these two units is indistinct. Moore et al.

(2017) interpreted the Bright, Pitted Uplands to be a formerly continuous deposit degraded either by sublimation or by undermining and collapse, possibly through basal melting. We hypothesize that the bladed terrain may represent a relatively well-preserved form of this deposit that has only undergone either of these processes (or maybe a combination of them), while the Bright, Pitted Uplands represent a portion that has subsequently been extensively mantled and modified by N_2 ice glaciation. The CH_4 signature of the bladed terrain and the pit crests in the Bright, Pitted Uplands may be indicative of the composition of this same deposit; this would be consistent with an origin of the pitted and bladed textures through sublimation of CH_4 ice. However, we cannot discount the possibility that the CH_4 signature is at least partly caused by recent condensation of atmospheric CH_4 ice onto the crests of pits and blades, in which case both the N_2 and CH_4 mantles would mask the true compositional identity of the underlying deposit. The aligned NW-SE orientation of clusters of relatively large pits (several kilometers across, '3' labels in Fig. 13) implies that these pits have formed due to surface collapse above zones of regional, extensional tectonism. The genesis of these larger pits is therefore likely to be distinct from that of the smaller pits that characterize the Bright, Pitted Uplands.

5. Stratigraphy and Geologic History of Sputnik Planitia

5.1 Superposition relations

Fig. 15 presents a correlation of the geological units mapped in Fig. 5. All mapped units are interpreted to either consist of, or to be presently experiencing modification by, low-viscosity N_2 ice, which is easily mobilized at Pluto surface thermal conditions. As such, all mapped units (with the exception of the Pre-Sputnik Planitia Uplands) are interpreted to be experiencing resurfacing to some degree in the present day. Given the almost total absence of impact craters from these units, assembling a chronology for them is challenging, but observations of superposition relations aid in constructing a

relative stratigraphy. An absolute age scale accompanies the correlation in Fig. 15, and as we discuss in section 5.2, absolute ages for units can be estimated based on considerations of crater counts performed for the uplands surrounding Sputnik Planitia (relevant to the Bright, Pitted Uplands), and for the Sputnik Planitia plains units, considerations of climatic variations tied to Pluto's obliquity cycles, as well as the timescale of convection of N_2 ice.

The Bright, Pitted Uplands and the Bright, Chaotic Terrain are each bordered by only two units: the Pre-Sputnik Planitia Uplands and, respectively, the Patchy, Pitted, Marginal Plains and the Chaotic, Inter-Block Material. Crosscutting relations indicate that these latter two units superpose the Bright, Pitted Uplands and the Bright, Chaotic Terrain respectively. Where the three units of the mountain ranges along the western edge of Sputnik Planitia (units abm, ibm and drt) contact the Pre-Sputnik Planitia Uplands, crosscutting relations show that they are always superposing the Pre-Sputnik Planitia Uplands. Within this suite of three units, the Chaotic, Inter-Block Material (unit ibm) tends to embay, and occupy angular interstitial spaces between, the Chaotic, Angular, Blocky Mountains (unit abm), indicating that the Chaotic, Inter-Block Material is stratigraphically higher than the Chaotic, Angular, Blocky Mountains. The Dark, Ridged Terrain (unit drt) appears to represent dark material covering the Chaotic, Inter-Block Material, and so is stratigraphically higher than both the Chaotic, Inter-Block Material and the Chaotic, Angular, Blocky Mountains. With the exception of Columbia Colles, the Scattered Hills (unit sh) are always completely embayed by various plains units of Sputnik Planitia. Columbia Colles crosscuts the contact between the plains and the Pre-Sputnik Planitia Uplands, indicating that the Scattered Hills are stratigraphically higher than the Pre-Sputnik Planitia Uplands.

The eight plains units of Sputnik Planitia (units bcp, dcp, tbp, spp, dpp, lpp, pmp, and dmp) embay and superpose all of the aforementioned units whenever they contact them, and as such are located at the top of the stratigraphic column. Proximal to the main contact between the Bright, Cellular Plains (unit bcp) and the Dark, Cellular Plains (unit dcp), the Bright, Cellular Plains are observed to embay enclaves of the Dark, Cellular Plains that are located within the interiors of cells, while at the contact itself, the

Bright, Cellular Plains are observed to intrude into the Dark, Cellular Plains along the paths of troughs that separate cells. While we interpret the higher albedo of the Bright, Cellular Plains to be caused by a thin mantle of pure N_2 ice that has condensed onto the plains here, the cellular pattern of the plains is continuous and unperturbed across this contact. This implies that the Bright, Cellular Plains and Dark, Cellular Plains are both formed from the same convecting N_2 ice mass and that they are essentially contemporaneous in age. The relation between the Dark, Cellular Plains and the Dark, Trough-Bounding Plains (unit tbp) is complex: both units can embay each other in different instances, and the two may also be stratigraphically contemporaneous.

The contact between the Bright, Cellular Plains and the various non-cellular plains units in southern Sputnik Planitia is interpreted to represent the transition zone between the northern portion of Sputnik Planitia where the combination of N_2 ice depth and basal heat flow is conducive to convection, and the southern portion where the conditions are not conducive to convection. Within the non-cellular plains proximal to the contact, there are several instances of individual cells, as well as clusters of cells, being surrounded or nearly surrounded by the non-cellular plains. Within the cellular plains, there are also areas of non-cellular plains situated interstitially between cells. The planforms of the cells are consistently ovoid while the interstitial non-cellular plains are always angular. We interpret this configuration between the Bright, Cellular Plains and the various non-cellular plains to indicate that the former are stratigraphically higher than the latter, whereby the continuous convective mobilization of the N_2 ice within the Bright, Cellular Plains causes the cells to infringe upon and incorporate relatively immobile N_2 ice within the non-cellular plains.

Within the non-cellular plains (comprising units spp, dpp, lpp, pmp, and dmp), the configurations of contacts between different units tend to be highly complex, especially where they occur in-between the Bright, Cellular Plains and the Bright, Pitted Uplands. Units can be seen to both embay and also be embayed by the other units, and it is not generally clear which is superposing the other. Assessing the significance of the crosscutting and embayment relations between these units in terms of assigning a

chronology to them is challenging due to the fact that we interpret them to represent various forms of modification (involving some combination of flow, sublimation, and/or mantling) of the non-convecting portion of the N_2 ice mass in southern Sputnik Planitia, rather than separate deposits that have been sequentially laid down onto the surface. As such, the formation of these various units is dependent on factors (in particular the stress applied to the N_2 ice) that are not necessarily confined to a particular era in time, and they can essentially be regarded as developing concurrently.

5.2 Geological history

The most ancient feature (rather than specific unit) within the mapping area is the ~1300 by ~1000 km basin in which Sputnik Planitia is located. This feature is hypothesized to be an impact basin, despite its irregular shape: Caloris Planitia on Mercury is an impact basin of comparable diameter that also deviates significantly from circularity (Schenk et al., 2015). The appearance of this basin has been instrumental in governing the behavior of N_2 ice on Pluto's surface. Due to Pluto's high obliquity and the likelihood that the basin reaches a depth of several kilometers, its low-latitude position would enhance its status as a cold trap for N_2 ice (Hamilton et al., 2016; Earle et al., 2017). Climate modeling indicates that the great majority of N_2 ice on Pluto would migrate to and be sequestered within the basin within 10,000 terrestrial years of its formation (Bertrand and Forget, 2016). Since then, the action of flowing and convecting N_2 ice has been instrumental in modifying the rim to varying degrees around its circumference. The topographic expression of the southern portion of the rim is in fact non-existent, which may be due to it having been eroded away by glacial flow of N_2 ice over the last 4 Gyrs, or alternatively due to it having never existed as a consequence of the obliqueness of the angle of impact that formed the basin.

Crater counts by Moore et al. (2016) indicate an age for the Bright, Pitted Uplands not exceeding ~2 Gyrs (for craters ~40 km diameter), but condensation of N_2 ice onto the landscape and its subsequent transportation into Sputnik Planitia by glacial flow may well have been modifying this unit continuously

for the last few Gyrs up until the present day. The pitted texture of the unit is reminiscent of that of the bladed terrain to the east of the mapping area (Moore et al., 2016; 2017), which the Bright, Pitted Uplands may represent a strongly modified version of. At some point after their formation, the Bright, Pitted Uplands were subjected to regional-scale extension, resulting in NE-SW-aligned troughs and normal faults that have since been extensively degraded by the action of N_2 ice upon the landscape.

The mountainous units, including the Chaotic, Angular, Blocky Mountains, the Chaotic, Inter-Block Material, and the Dark, Ridged Terrain, are interpreted to display the oldest surfaces of any Sputnik Planitia unit. This mountainous material is interpreted to be H_2O ice-rich crustal fragments that have become dislodged from the Pre-Sputnik Planitia Uplands to the west of Sputnik Planitia by a combination of extensional fracturing and intrusion by denser, flowing N_2 ice. Both of these processes may presently be affecting the Bright, Chaotic Terrain at the northwestern margin of Sputnik Planitia, which appears to represent tectonized Pre-Sputnik Planitia Uplands terrain that has been partly covered by N_2 ice of Sputnik Planitia, and which will eventually fragment to transform into the Sputnik Planitia mountainous material. Crater counts for the Pre-Sputnik Planitia Uplands to the north of Sputnik Planitia (to which the Bright, Chaotic Terrain belongs) indicate an age that is slightly younger than the LHB, i.e. almost 4 Gyr (Moore et al., 2016). So while the Bright, Chaotic Terrain may be currently undergoing extensive modification, some portions of it may still date from the immediate post-LHB era (such as the dark peaks between the N_2 ice-covered valleys). This principle also applies when attempting to determine the age of the mountainous material itself. There is uncertainty as to when and over what duration the mountains became separated from the Pre-Sputnik Planitia Uplands. The angular planforms and often sheer and steep faces that characterize many mountains may suggest that they have broken away relatively 'recently', i.e. recently enough not to have developed rounded and roughened morphologies due to mass wasting and abrasion resulting from contact with other mountains within the ranges. Despite this, some larger mountain blocks display faces that have a texture that is comparable to that of the surrounding Pre-Sputnik Planitia Uplands that date almost to the LHB (Moore et al., 2016), meaning that the timing of the

earliest break-up of the surrounding Pre-Sputnik Planitia Uplands to form the mountains can realistically only be constrained to an almost 4 Gyr period stretching from just after the LHB to the present day. We can assert that the Dark, Ridged Terrain formed later than any of the other mountainous units, as it comprises dark material resting on top of the Chaotic, Inter-Block Material, although exactly when this material was emplaced, and over what timescale it developed its ridged texture, is unknown.

Unlike these mountains of western Sputnik Planitia, most of which have remained grounded in ranges in shallow parts of the Planitia for an unknown period of time, the Scattered Hills have instead been rafted into eastern Sputnik Planitia by glacial flow of N_2 ice after having been eroded from the Bright, Pitted Uplands in east Tombaugh Regio. Because many of these small hills are interpreted to be floating within the N_2 ice (with the exception of those within Challenger and Columbia Colles), their transport into Sputnik Planitia will have occurred on a timescale corresponding to the flow rate of the N_2 glaciers, which may be measured in terms of terrestrial centuries (Umurhan et al., 2017). But as with the western mountains, surfaces on some of the hills may well date back as far as that of the Bright, Pitted Uplands from which they were derived, i.e. ~2 Gyrs.

Numerical modeling of sluggish lid convection indicates that for most cells within the cellular plains, the surface ice at the center of a given upwelling can be transported to the downwelling perimeter on a timescale of ~500,000 terrestrial years (McKinnon et al., 2016). As such, this is the upper limit we place on the age of the cellular plains. The rapid rate of surface renewal in the cellular plains is effective in limiting the size to which sublimation pits can grow to only a few hundred meters across. The location of the boundary between the Bright and Dark, Cellular Plains changes according to the precession of the Arctic Circle with Pluto's 2.8 million terrestrial year obliquity cycles, which affects which parts of Sputnik Planitia are zones of net N_2 ice sublimation, and which are zones of net N_2 ice condensation. The cycle is currently advancing towards a moderate obliquity (of 127°) that will be reached in 600,000 terrestrial years. Over this time, the northern boundary of the bright mantle that characterizes the Bright,

Cellular Plains as well as the Bright, Pitted Uplands would be expected to advance northwards from the present 30°N to 37°N.

As described in section 5.1, constraining the chronology of the non-cellular plains units based on their complex embayment relations is challenging. Beyond superposition relations, the pit sizes exhibited by different units could potentially provide a clue as to their ages. For instance, the wider and deeper pits exhibited by the Deeply Pitted Plains compared to those within the cellular plains may be taken to indicate that the Deeply Pitted Plains have not been resurfaced as recently as the cellular plains, due to the absence of convection allowing the sublimation pits to grow to larger sizes. However, this interpretation does assume that a uniform rate of sublimation is forming pits across all units. Moore et al. (2017) remark that their initial modeling of pit formation suggests that evolution of the pits can be sporadic, with extended periods of relative inactivity interrupted by short bursts of rapid sublimation. It is possible that the latter has affected the Deeply Pitted Plains, in the form of shearing of the N_2 ice to create incipient crevasses that are subsequently rapidly widened by sublimation, as has been suggested by Moore et al. (2017). The Sparsely Pitted Plains may represent an evolved version of the Lightly and Deeply Pitted Plains, whereby pit topography has been softened by creep of N_2 ice and perhaps also mantling by condensation of N_2 ice, yet there is ambiguity as to whether the present Lightly and Deeply Pitted Plains are currently undergoing transformation into the Sparsely Pitted Plains, or whether the Lightly and Deeply Pitted Plains are currently forming within preexisting Sparsely Pitted Plains. Evidence for active flow within the non-cellular plains includes the wavelike patterns created by swarms of these pits in the Deeply Pitted Plains, as well as the flow lines of the valley glaciers in the Patchy, Pitted, Marginal Plains. Patches of what appear to be remnant N_2 ice plains filling impact craters and valleys in a few locations within the Pre-Sputnik Planitia Uplands represent evidence that cycles of advance and retreat of glacial N_2 ice have affected surfaces here, with the plains advancing to maximum coverage during periods of extreme obliquity, and therefore maximum atmospheric pressure. These conditions were last reached 840,000 terrestrial years ago. Given the ambiguity associated with defining the stratigraphy of the non-

cellular plains units, we choose to adopt an estimate of 840,000 terrestrial years as a general upper age limit for them, as they will have all been retreating from the Pre-Sputnik Planitia Uplands since then. This is at least until new research focusing on the rheological properties of N_2 ice at Pluto surface conditions yields a better understanding of how the timescale of its sublimation may be affected by various processes, and whether such processes are even feasible in N_2 ice, such as shearing.

6. Conclusion

For its size, the mapped area of Pluto incorporating Sputnik Planitia and its surroundings is perhaps unique within the outer Solar System for displaying such a wide array of geological units that present a great range of surface ages. Our mapping has focused on the terrains within this area that are presently being modified to some extent by the actions of mobilized N_2 ice, whether through flow, sublimation, or glacial erosion. The vast N_2 ice plains of Sputnik Planitia are in a constant state of renewal even 4.5 Gyrs after Pluto's formation, while intrusion into, and mantling of, portions of the surrounding highlands terrain by N_2 ice has been instrumental in defining their appearance. Pluto's orbital and physical characteristics are important factors that contribute to the diversity and activity of the geology in and around Sputnik Planitia. The distant location of Pluto's orbit in the Solar System is where conditions are such that exotic compounds such as N_2 and CH_4 can exist in abundance as solids on the surface. These compounds are nevertheless volatile enough such that they can be readily mobilized by the radiogenic heat that still emanates from Pluto's interior (in the case of the N_2 ice in Sputnik Planitia) or by the profound insolation and climatic changes that take place across Pluto's 2.8 Myr obliquity cycle (in the case of sublimation and re-deposition, and glacial advance and retreat, of N_2 ice). This map represents the first step in what we intend to be a mapping project that encompasses the entirety of the well-resolved encounter hemisphere on Pluto. While Sputnik Planitia is contained entirely within the present mapping area, the Pre-Sputnik Planitia Uplands extend beyond the boundaries of the map, and detailed

characterization of the various units that form this terrain further afield across Pluto's surface will reveal information about the degree to which volatile mobilization has affected Pluto in settings that are far removed from Sputnik Planitia.

Acknowledgements

The authors gratefully acknowledge the support of the NASA New Horizons mission (within the New Frontiers program) and the NASA Postdoctoral Program in facilitating this work. We also acknowledge the helpful and constructive comments provided by the two reviewers of the manuscript.

References

Barr, A.C., McKinnon, W.B., 2007. Convection in ice I shells and mantles with self-consistent grain size. *J. Geophys. Res. Planets*, **112**, E02012, doi:10.1029/2006JE002781.

Bertrand, T., Forget, F., 2016. Observed glacier and volatile distribution on Pluto from atmosphere-topography processes. *Nature*, doi:10.1038/nature19337.

Binzel, R.P., Earle, A.M., Young L.A., Stern, S.A., Olkin, C.B., Ennico, K., Moore, J.M., Grundy, W., Weaver, H.A., and the New Horizons Geology and Geophysics Imaging Team, 2017. Climate zones on Pluto and Charon. *Icarus*, doi:10.1016/j.icarus.2016.07.023.

Buratti, B.J., Hofgartner, J.D., Hicks, M.D., Weaver, H.A., Stern, S.A., Momary, T., Mosher, J.A., Beyer, R.A., Verbiscer, A.J., Zangari, A.M., Young, L.A., Lisse, C.M., Singer, K., Cheng, A., Ennico, K.,

Olkin, C.B., 2017. Global albedos of Pluto and Charon from LORRI New Horizons observations. *Icarus*, doi:10.1016/j.icarus.2016.11.012.

Cheng, A.F., et al., 2008. Long-Range Reconnaissance Imager on New Horizons. *Space Sci. Rev.* **140,** 189–215, doi:10.1007/s11214-007-9271-6.

Dobrovolskis, A.R., Harris, A.W., 1983. The obliquity of Pluto. *Icarus*, **55**, 231-235.

Dobrovolskis, A.R., Peale, S.J., Harris, A.W., 1997. Dynamics of the Pluto-Charon binary. In: Stern, S.A., Tholen, D.J. (Eds.), Pluto and Charon, University of Arizona Press, Tucson, AZ, pp. 159-192.

Earle, A.M., Binzel, R.P., 2015. Pluto's insolation history: Latitudinal variations and effects on atmospheric pressure. *Icarus*, **250**, 405-412, doi:10.1016/j.icarus.2014.12.028.

Earle, A.M., Binzel, R.P., Young, L.A., Stern, S.A., Ennico, K., Grundy, W., Olkin, C.B., Weaver, H.A., and the New Horizons Geology and Geophysics Imaging Team, 2017. Long-term surface temperature modeling of Pluto. *Icarus*, doi:10.1016/j.icarus.2016.09.036.

Forget, F., Bertrand, T., Vangvichith, M., Leconte, J., Millour, E., Lellouch, E., 2017. A post-New Horizons global climate model of Pluto including the N_2, CH_4 and CO cycles. *Icarus*, doi:10.1016/j.icarus.2016.11.038.

Gladstone, G.R., et al., 2016. The atmosphere of Pluto as observed by New Horizons. *Science*, **351**, aad8866, doi:10.1126/science.aad8866.

Grundy, W.M., et al., 2016. Surface compositions across Pluto and Charon. *Science*, **351**, aad9189, doi:10.1126/science.aad9189.

Hamilton, D.P., Stern, S.A., Moore, J.M., Young, L.A., and the New Horizons Geology, Geophysics and Imaging Theme Team, 2016. The rapid formation of Sputnik Planitia early in Pluto's history. *Nature*, doi:10.1038/nature20586.

Hapke, B., 1993. *Theory of Reflectance and Emittance Spectroscopy* (Cambridge University Press, NY).

van Hemelrijck, E., 1982. The insolation at Pluto. *Icarus*, **52**, 560-564.

Howard, A.D., et al., 2017. Present and past glaciation on Pluto. *Icarus*, doi:10.1016/j.icarus.2016.07.006.

Hussmann, H., Sohl, F., Spohn, T., 2006. Subsurface oceans and deep interiors of medium-sized outer planet satellites and large trans-neptunian objects. *Icarus*, **185**, 258-273, doi:10.1016/j.icarus.2006.06.005.

Malin, M.C., Edgett, K.S., 2000. Rough is smooth and smooth is rough: The Martian surface at meter scale versus hectomoeter scales and implications for future landing sites. *Lunar Planet. Sci. Conf XXXI*, Abstract #1059.

McKinnon, W.B., Simonelli, D.P., Schubert, G., 1997. Composition, internal structure, and thermal evolution of Pluto and Charon. In: Stern, S.A., Tholen, D.J. (Eds.), Pluto and Charon, University of Arizona Press, Tucson, AZ, pp. 295-346.

McKinnon, W.B., et al., 2016. Convection in a volatile nitrogen-ice-rich layer drives Pluto's geological vigour. *Nature*, **534**, 82-85, doi:10.1038/nature18289.

Moore, J.M., Wilhelms, D.E., 2001. Hellas as a possible site of ancient ice-covered lakes on Mars. *Icarus*, **154**, 258-276, doi:10.1006/icar.2001.6736.

Moore, J.M., et al., 1999. Mass movement and landform degradation on the icy Galilean satellites: Results of the Galileo nominal mission. *Icarus*, **140**, 294-312.

Moore, J.M., et al., 2016. The geology of Pluto and Charon through the eyes of New Horizons. *Science*, **351**, aad7055, doi:10.1126/science.aad7055.

Moore, J.M., et al., 2017. Sublimation as a landform-shaping process on Pluto. *Icarus*, doi:10.1016/j.icarus.2016.08.025.

Nimmo, F., et al., 2016. Reorientation of Sputnik Planitia implies a subsurface ocean on Pluto. *Nature*, doi:10.1038/nature20148.

Petrenko, V.F., Whitworth, R.W., 1999. *Physics of Ice*, Oxford Univ. Press, Oxford.

Protopapa, S., et al., 2017. Pluto's global surface composition through pixel-by-pixel Hapke modeling of New Horizons Ralph/LEISA data. *Icarus*, doi:10.1016/j.icarus.2016.11.028.

Schenk, P.M., Nimmo, F., McKinnon, W.B., Moore, J.M., Ennico, K., Stern, S.A., Olkin, C., Young, L.A., Weaver, H., and the New Horizons Science Team, 2015. A large impact origin for Sputnik Planum and surrounding terrains, Pluto? *AAS DPS 47th Annual Meeting,* Abstract 200.06.

Schmitt, B., et al., 2017. Physical state and distribution of materials at the surface of Pluto from New Horizons LEISA imaging spectrometer. *Icarus*, doi:10.1016/j.icarus.2016.12.025.

Scott, T.A., 1976. Solid and liquid nitrogen. Phys. Rep., **27**, 89-157, doi:10.1016/0370-1573(76)90032-6.

Stern, S.A., et al., 2015. The Pluto system: Initial results from its exploration by New Horizons. *Science*, **350**, aad1815-1-7.

Stern, S.A., et al., 2017. Past epochs of significantly higher pressure atmospheres on Pluto. *Icarus*, doi:10.1016/j.icarus.2016.11.022.

Tanaka, K.L., Skinner, J.A., Hare, T.M., 2011. Planetary Geologic Mapping Handbook, USGS, Flagstaff, AZ.

Trowbridge, A.J., Melosh, H.J., Steckloff, J.K., Freed, A.M., 2016. Vigorous convection as the explanation for Pluto's polygonal terrain. *Nature*, **534**, 79-81, doi:10.1038/nature18016.

Umurhan, O.M., et al., 2016. An expanded analysis of nitrogen ice convection in Sputnik Planum. *AAS DPS 48th Annual Meeting*, Abstract 213.06.

Umurhan, O.M., et al., 2017. Modeling glacial flow on and onto Pluto's Sputnik Planum. Submitted to Icarus.

Weaver, H.A., Gibson, W.C., Tapley, M.B., Young, L.A., Stern, S.A., 2008. Overview of the New Horizons science payload. *Space Sci. Rev*. **140,** 75–91, doi:10.1007/s11214-008-9376-6.

White, O.L., Umurhan, O.M., Moore, J.M., Howard, A.D., 2016. Modeling of ice pinnacle formation on Callisto. *J. Geophys. Res. Planets*, **121**, pp. 21-45, doi:10.1002/2015JE004846.

Wilhelms, D.E., 1972. Geologic mapping of the second planet, *U.S. Geol. Surv., Interagency Report, Astrogeology*, **55**.

Wilhelms, D.E., 1990. Geologic mapping, in *Planetary Mapping*, edited by R. Greeley and R.M. Batson, Cambridge Univ. Press, New York, 208-260.

Yamashita, Y., Kato, M., Arakawa, M., 2010. Experimental study on the rheological properties of polycrystalline solid nitrogen and methane: implications for tectonic processes on Triton. *Icarus*, **207**, 972-977, doi:10.1016/j.icarus.2009.11.032.

Figures

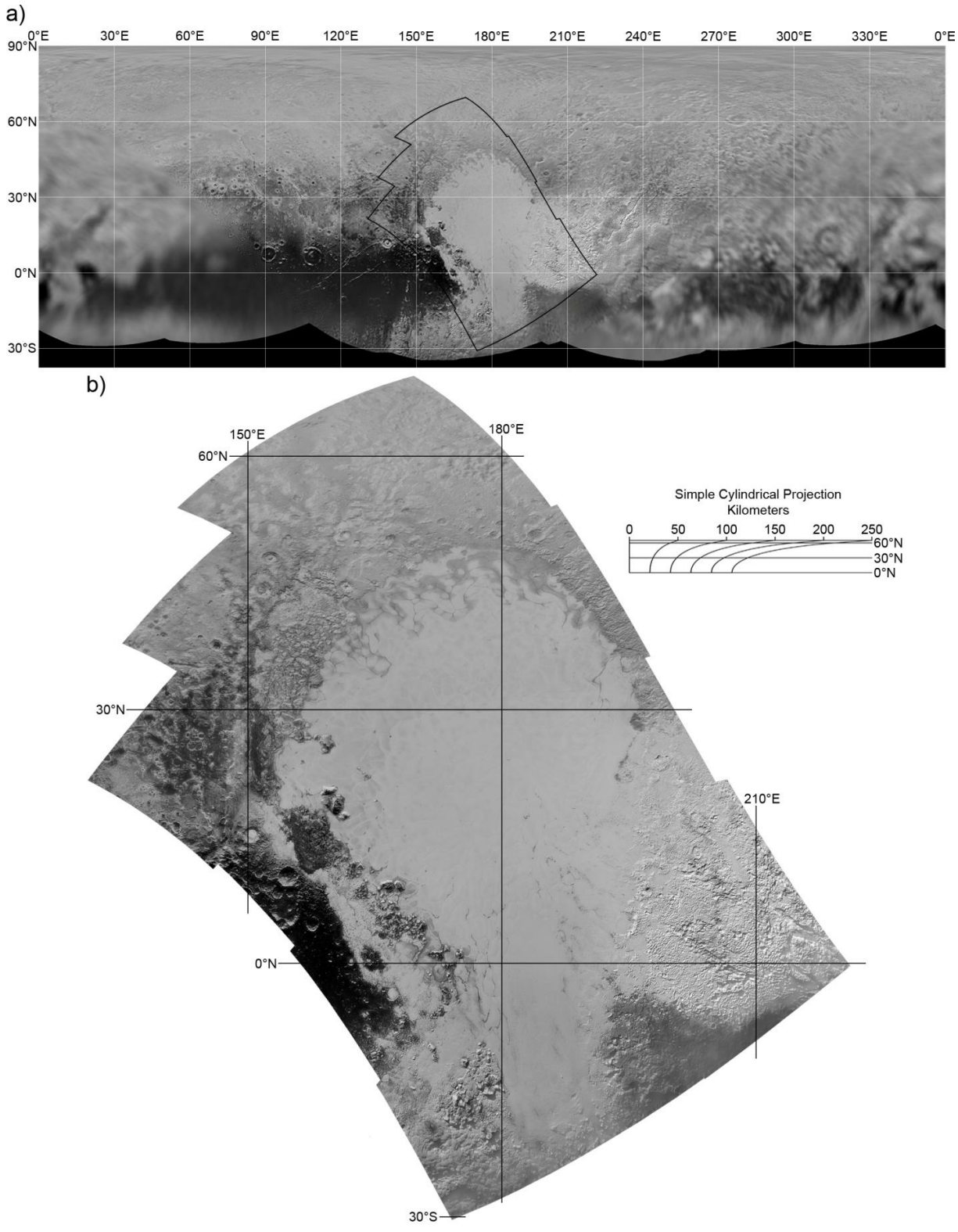
a)
0°E
30°E
60°E
90°E
120°E
150°E
180°E
210°E
240°E
270°E
300°E
330°E
0°E
90°N
60°N
30°N
0°N
30°S
b)
150°E
180°E
60°N
30°N
210°E
0°N
30°S
Simple Cylindrical Projection
Kilometers
0
50
100
150
200
250
60°N
30°N
0°N

Figure 1. A global, simple cylindrical, photometrically equilibrated mosaic of LORRI images of Pluto is shown in (a). Latitudes south of ~30°S were in darkness during the New Horizons flyby. The mapping area (comprising a mosaic of 12 LORRI images obtained at 386 m/pixel) is highlighted by the black boundary and is expanded in (b).

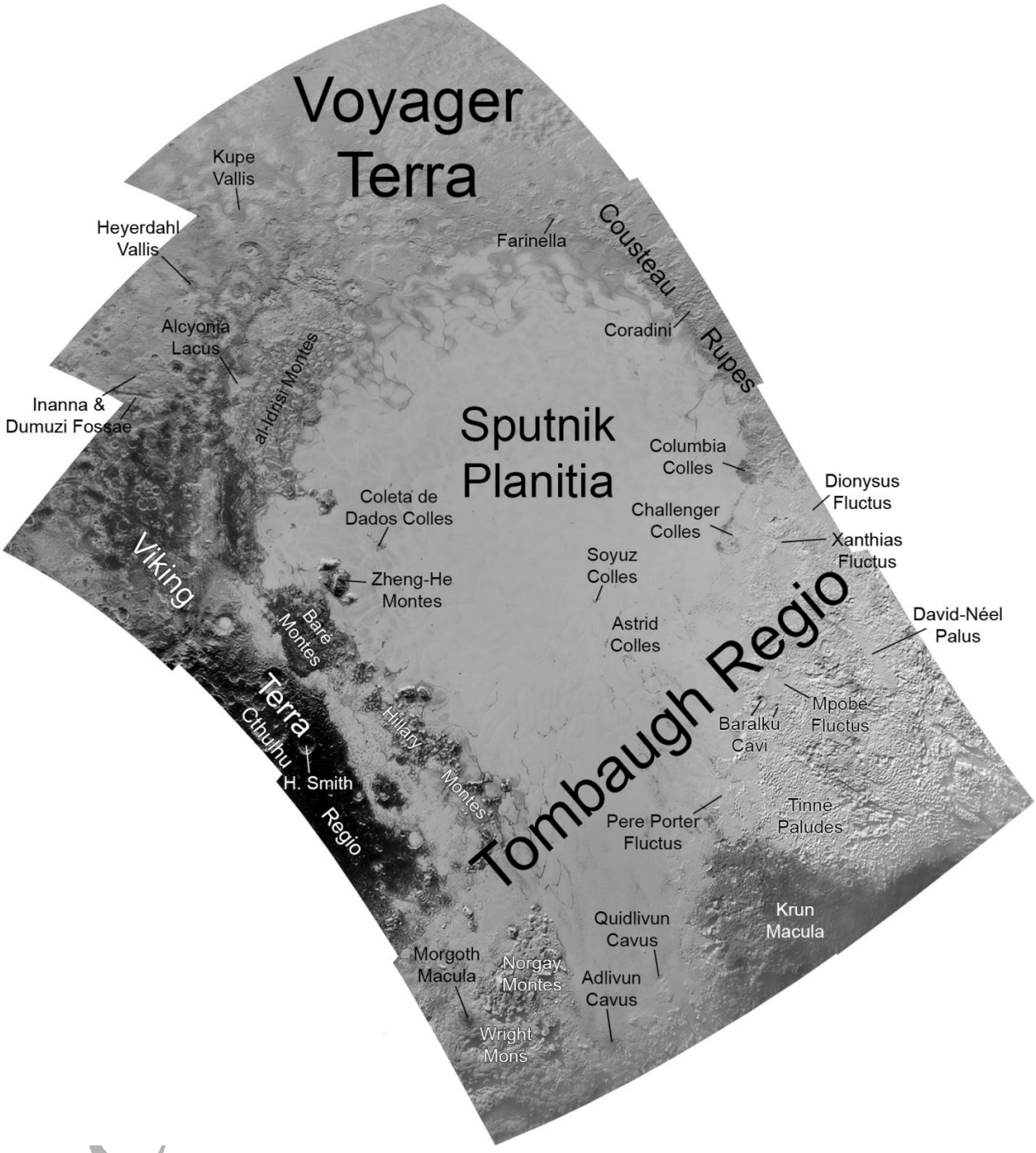

Figure 2. Informal nomenclature map for the mapping area.

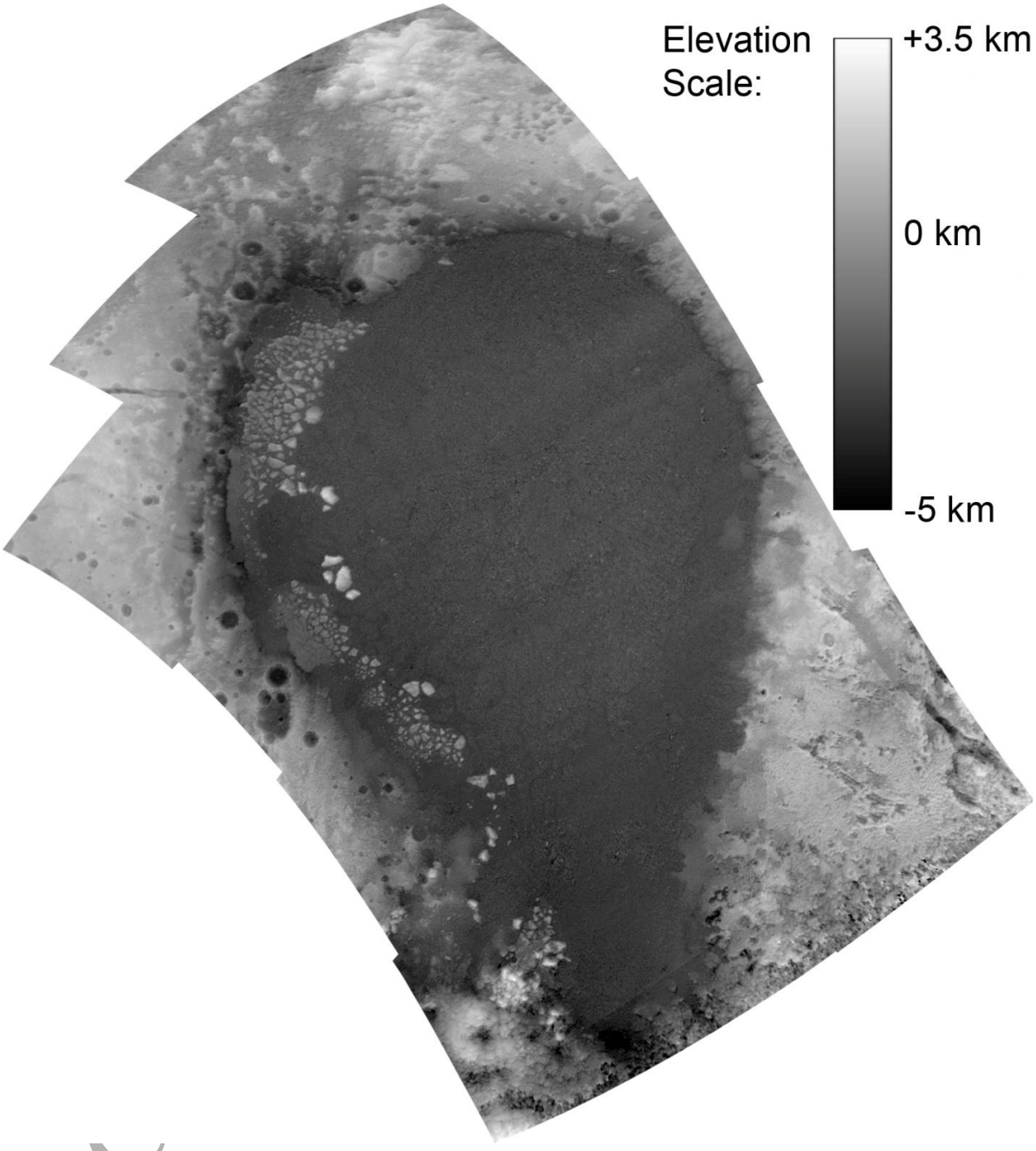

Figure 3. Stereo digital elevation model (DEM) of the mapping area. The data used to create the DEM include a mosaic of 15 LORRI frames obtained at a resolution of 386 m/pixel, and a single MVIC scan obtained at a resolution of 320 m/pixel. The DEM resolves features that are at least 1.9 km across and has a vertical precision of 115 m. NE-SW-aligned banding artifacts affect the DEM across Sputnik Planitia.

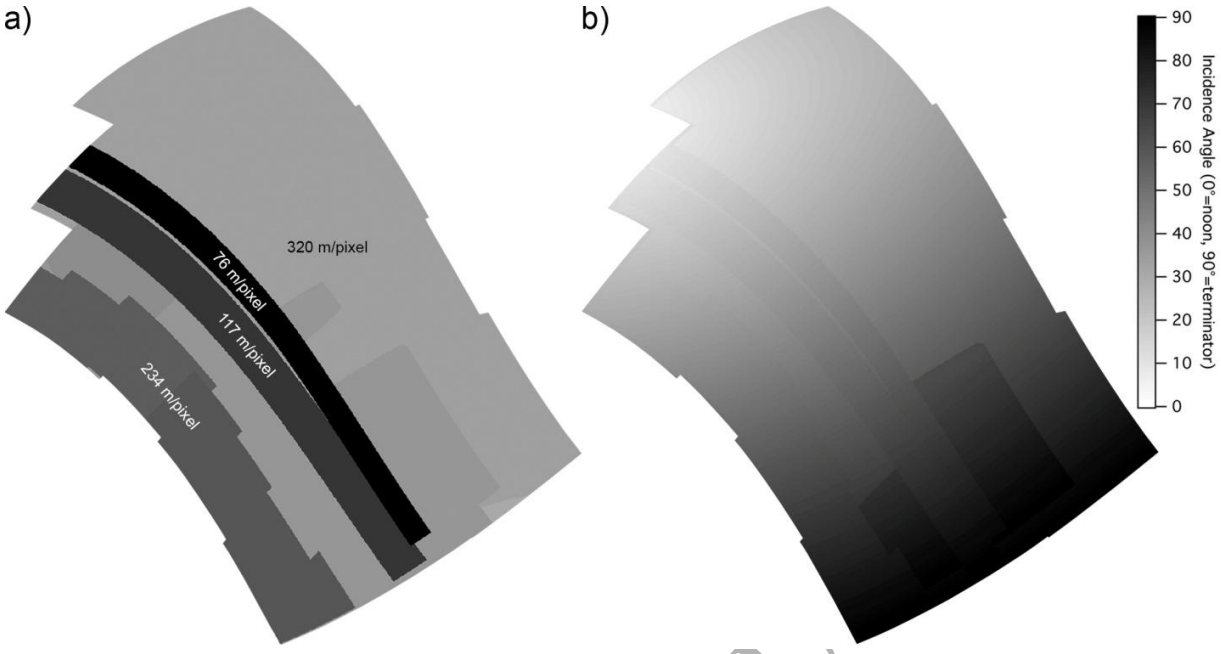

Figure 4. (a) Map of higher resolution New Horizons observations that coincide with the 386 m/pixel mapping base. 76 m/pixel strip is LORRI coverage obtained at a phase angle of 68.6°; 117 m/pixel strip is LORRI coverage obtained at a phase angle of 46.7°; 234 m/pixel strip is LORRI coverage obtained at a phase angle of 31.8°; the remainder of the map is 320 m/pixel MVIC coverage obtained at a phase angle of 67.9°. (b) Map of variation in solar incidence angle across the four observations shown in (a).

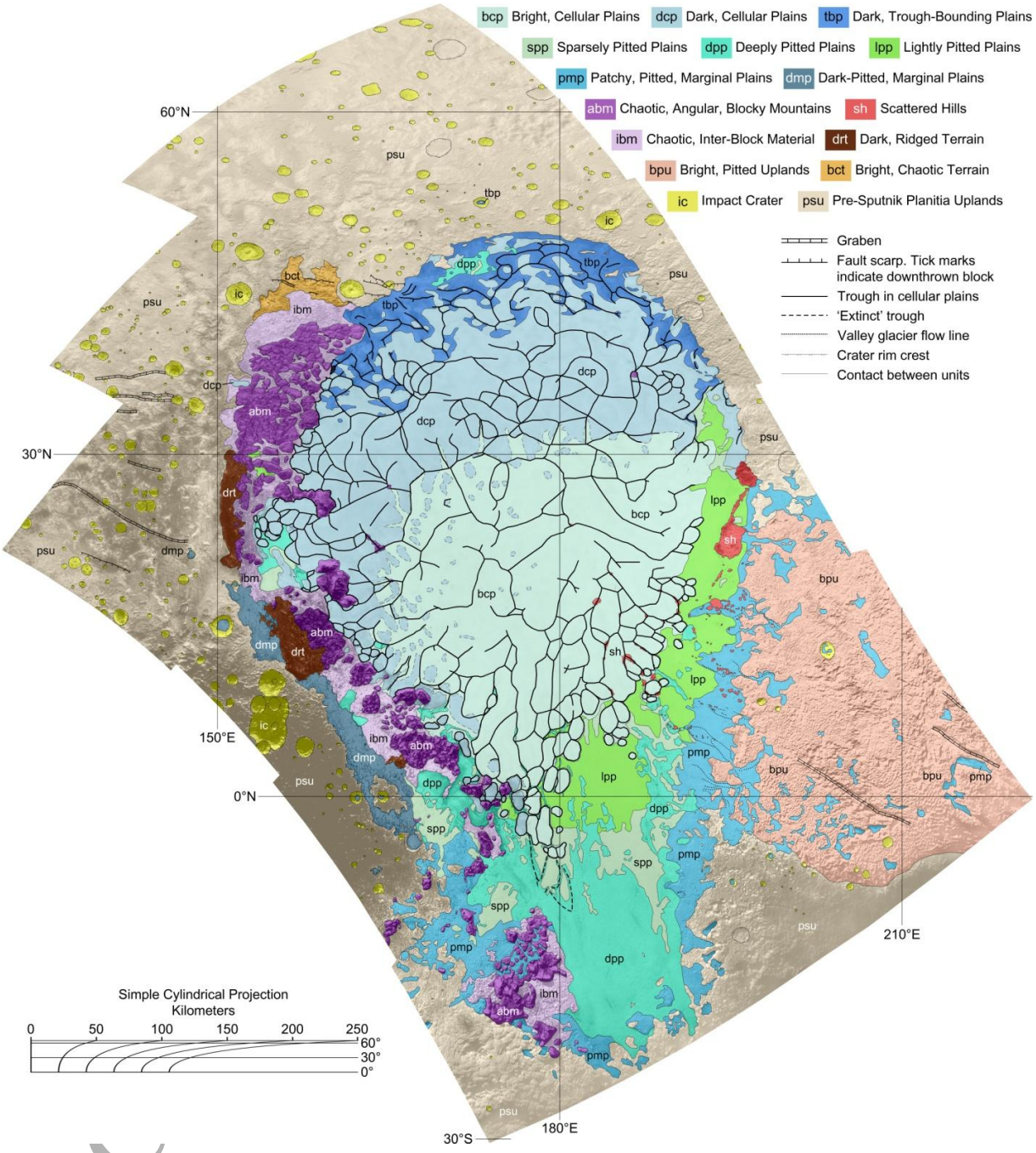

Figure 5. Geological map of the Sputnik Planitia region showing geological units identified by New Horizons image analyses. Map is overlain on photometrically equilibrated 386 m/pixel LORRI imagery. Upland terrains not currently directly affecting, or which are not currently affected by, Sputnik Planitia

are generalized as Pre-Sputnik Planitia Uplands (unit psu). Refer to Fig. 15 for a stratigraphic correlation of the map units.

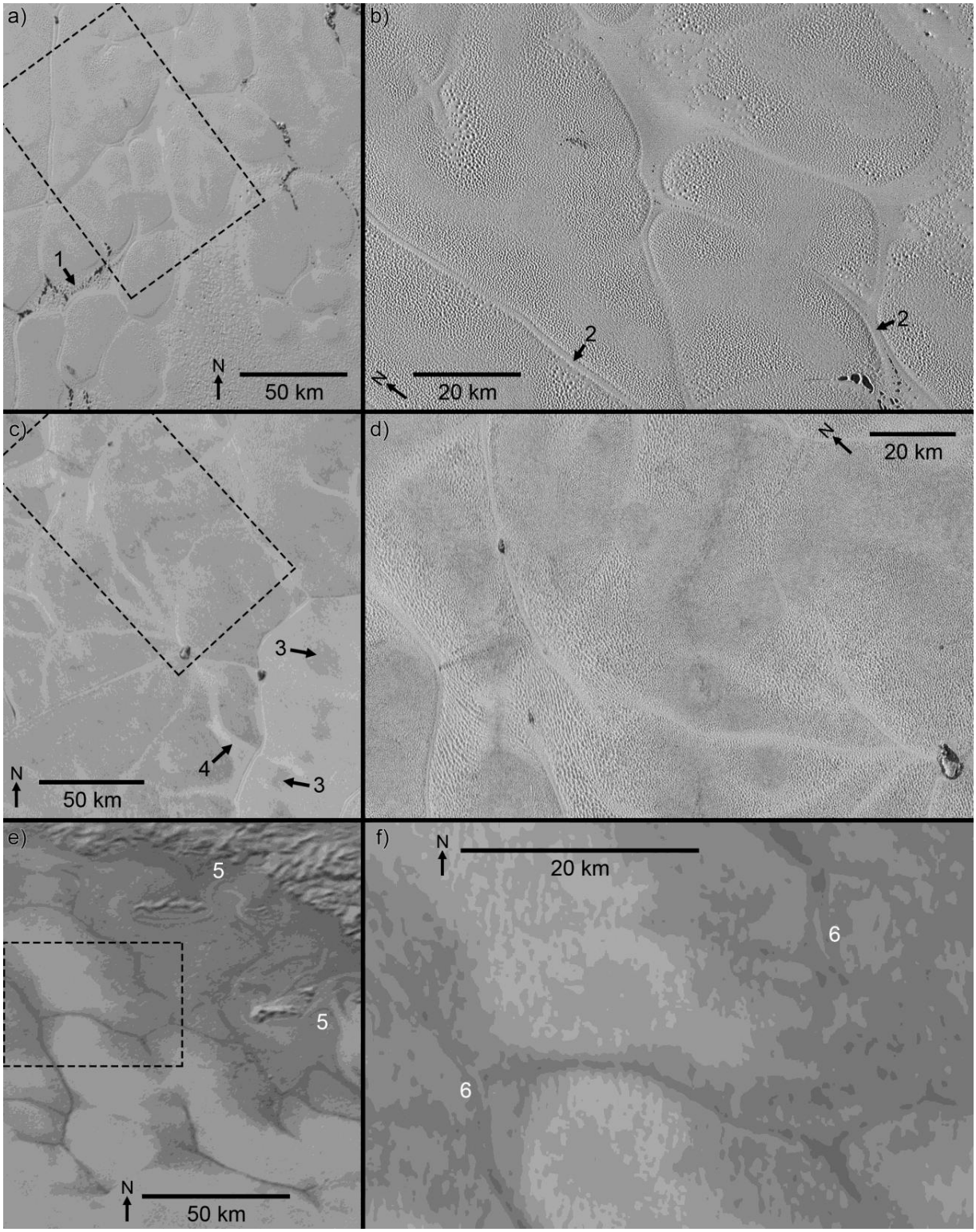
a)
1
N
50 km
b)
2
2
N
20 km
c)
3
4
3
N
50 km
d)
N
20 km
e)
5
5
N
50 km
f)
N
20 km
6
6

Figure 6. The three categories of cellular plains in Sputnik Planitia. (a) Bright, Cellular Plains (unit bcp). 320 m/pixel MVIC image, centered at 7.5°N, 182°E. Dashed box indicates the outline of the detail in (b). '1' label indicates an occurrence of the Deeply Pitted Plains (unit dpp) in-between cells. (b) Detail of the Bright, Cellular Plains in (a). 76 m/pixel LORRI image. '2' labels indicate broad medial ridges within troughs that mark cell boundaries. (c) Dark, Cellular Plains (unit dcp). 320 m/pixel MVIC image, centered at 28°N, 165°E. Dashed box indicates the outline of the detail in (d). '3' labels indicate enclaves of the Dark, Cellular Plains embayed by the Bright, Cellular Plains. '4' label indicates a 'filament' of Bright, Cellular Plains extending into the Dark, Cellular Plains. (d) Detail of the Dark, Cellular Plains in (c). 76 m/pixel LORRI image. (e) Dark, Trough-Bounding Plains (unit tbp). 386 m/pixel LORRI image, centered at 45.5°N, 182.5°E. Dashed box indicates the outline of the detail in (f). '5' labels indicate flow patterns between nunataks of the dissected plateau unit protruding out of the plains. (f) Detail of the Dark, Trough-Bounding Plains in (e). 320 m/pixel MVIC image. '6' labels indicate bright medial lineations at the dark boundaries of cells, interpreted to be medial ridges rising above dark material filling the troughs that define the boundaries.

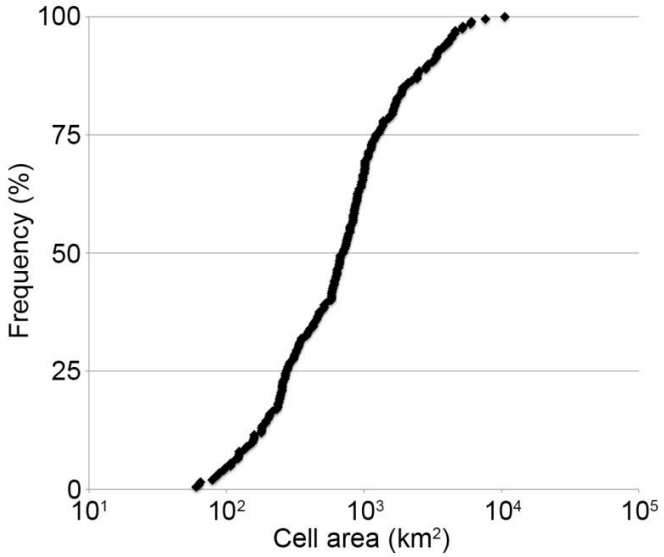

Figure 7. Cumulative size-frequency distribution chart of the areas of cells mapped in the cellular plains of Sputnik Planitia.

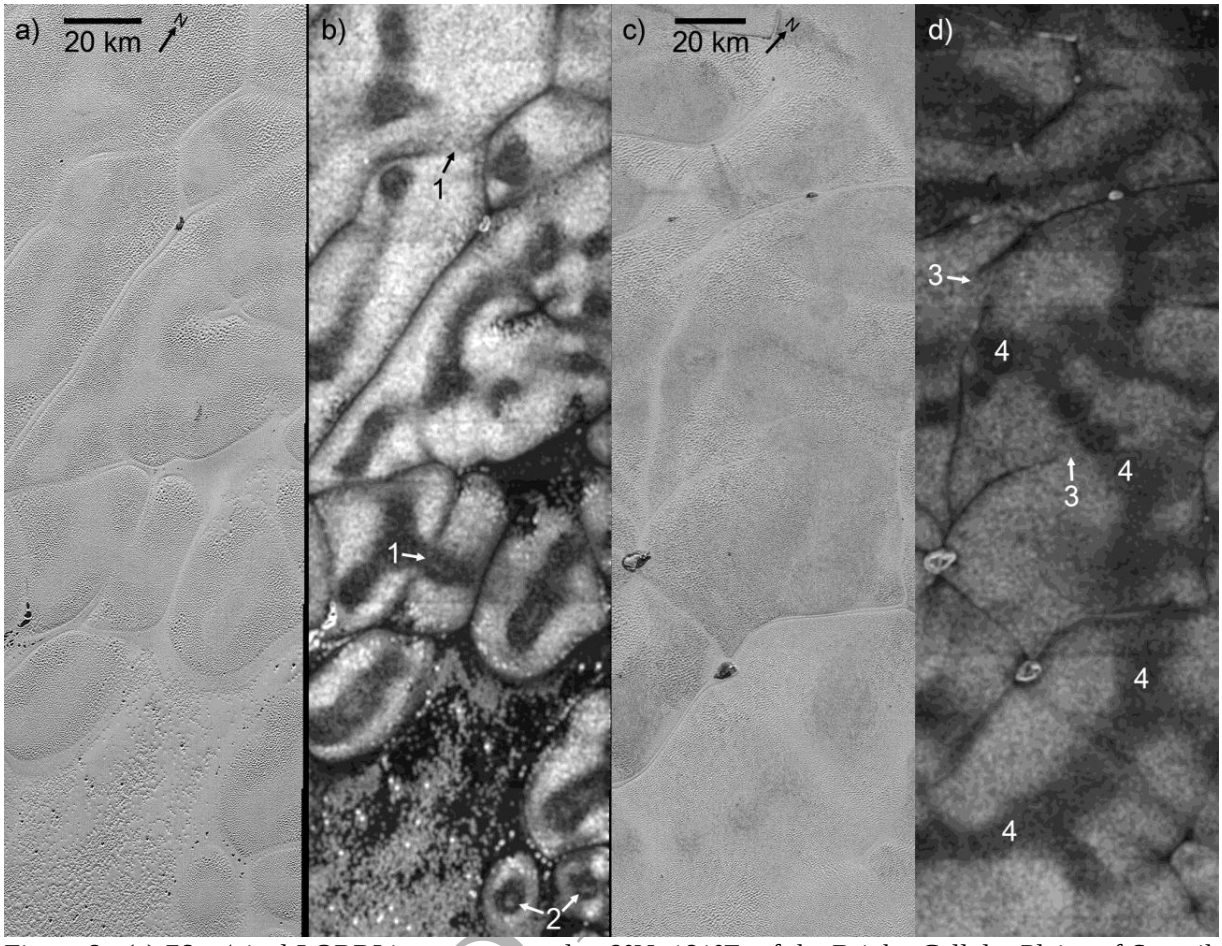

Figure 8. (a) 76 m/pixel LORRI image, centered at 9°N, 181°E, of the Bright, Cellular Plains of Sputnik Planitia, with non-cellular plains seen in the southern portion of the image. (b) Variance map covering the same area as in (a). The scaling of the variance map is arbitrary, but smooth (low variance) areas are dark, and rough (high variance) areas are bright. '1' labels indicate locations where troughs appear to be crosscut by pitted or smooth plains. '2' label indicates small cells displaying a 'bullseye' configuration in their surface texture. (c) (a) 76 m/pixel LORRI image, centered at 9°N, 181°E, of the Dark, Cellular Plains. (d) Variance map covering the same area as in (c). '3' labels indicate locations where cell boundaries appear to dissipate. '4' labels trace an arcuate network of smooth plains that extends across cell boundaries.

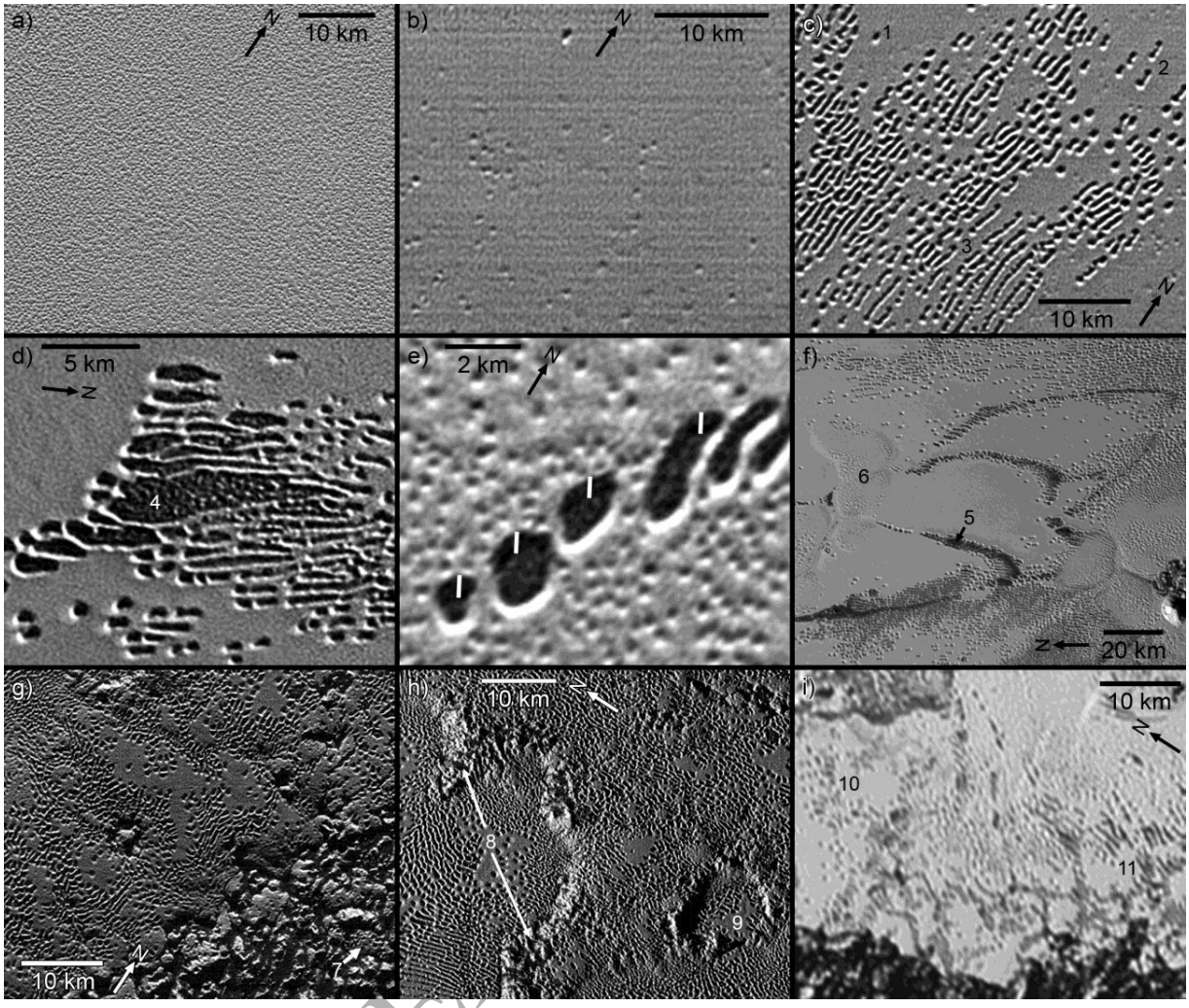

Figure 9. The five categories of non-cellular plains units in Sputnik Planitia. (a) Lightly Pitted Plains (unit lpp). 76 m/pixel LORRI image, centered at 1.5°N, 185°E. (b) Sparsely Pitted Plains (unit spp). 117 m/pixel LORRI image, centered at 7°S, 187.5°E. Isolated pits are seen scattered across the plains. The horizontally aligned texture in the image is an artifact. (c) Deeply Pitted Plains (unit dpp). 117 m/pixel LORRI image, centered at 6°S, 182.5°E. In this view, isolated pits ('1' label), doublets ('2' label), and chains of joined pits ('3' label) can be seen. (d) Deeply Pitted Plains with especially wide pits. Pit labeled '4' reaches 12 km long by 2.5 km across, and is large enough such that its low albedo, rubbly floor can be resolved. 76 m/pixel LORRI image, centered at 3.5°S, 187.5°E. (e) Deeply Pitted Plains featuring pits with shadows that are resolved in 76 m/pixel imagery, centered at 2.8°N, 186.5°E. White

lines indicate locations of shadow measurements. The Deeply Pitted Plains are surrounded by Lightly Pitted Plains. (f) 320 m/pixel MVIC image, centered at 7°S, 179.5°E, showing chains of wide (reaching several kilometers), joined pits with dark material covering their floors ('5' label) at the southern boundary of the Bright, Cellular Plains ('6' label). The chains form stretched, vaguely polygonal outlines. (g) Patchy, Pitted, Marginal Plains (unit pmp). 76 m/pixel LORRI image, centered at 9°S, 191.5°E. Pre-Sputnik Planitia Uplands occupy the lower right hand quadrant of the image, within which enclaves of the Patchy, Pitted, Marginal Plains are visible ('7' label at bottom right). (h) Patchy, Pitted, Marginal Plains exhibiting high relief akin to that of the adjacent Pre-Sputnik Planitia Uplands. '8' label indicates spurs extending into Sputnik Planitia; '9' label indicates an eroded, 12 km diameter impact crater. 76 m/pixel LORRI image, centered at 7.5°S, 190.5°E. (i) Dark-Pitted, Marginal Plains (unit dmp). '10' label indicates sub-km scale, equidimensional pits that are common amongst other Sputnik Planitia plains units; '11' label indicates low albedo, tendril-like features that cluster in groups and reach several km long. 234 m/pixel LORRI image, centered at 7°N, 160.5°E.

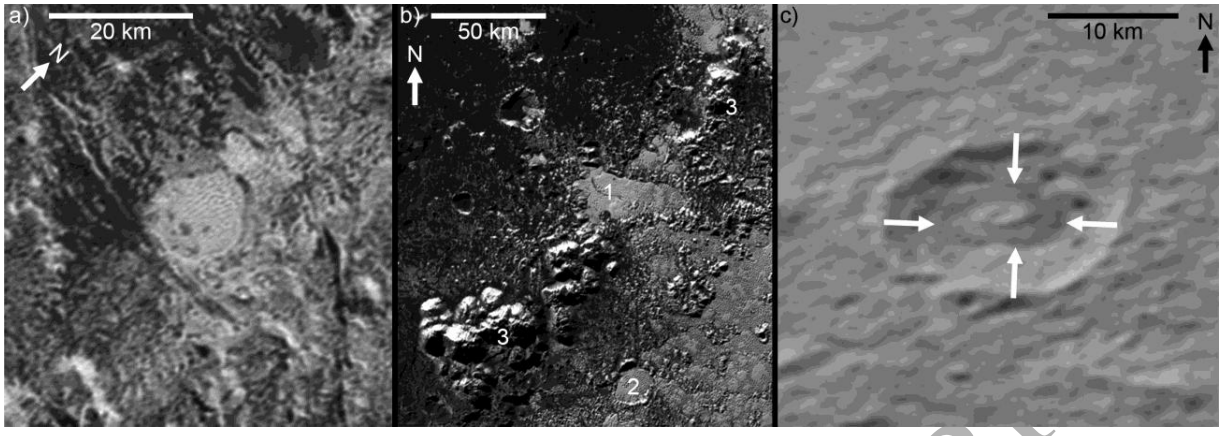

Figure 10. Three instances of ponded N_2 ice in depressions in the Pre-Sputnik Planitia Uplands beyond the western and northern borders of Sputnik Planitia. (a) Rimless, 13 km diameter impact crater located in a broad valley in Viking Terra, 103 km to the west of Sputnik Planitia. The Dark-Pitted, Marginal Plains cover the floor of the crater. 234 m/pixel LORRI image, centered at 21.5°N, 148°E. (b) Patchy, Pitted, Marginal Plains filling a valley ('1' label) and crater ('2' label) within the southern portion of Cthulhu Regio. The '3' labels indicate perched mountains of the Chaotic, Angular, Blocky Mountains unit. 234 m/pixel LORRI image, centered at 9.5°S, 165.5°E. (c) 18 km diameter impact crater located within Voyager Terra, 57 km to the north of Sputnik Planitia. Dark, Trough-Bounding Plains possibly cover the floor of the crater, surrounding a central peak protruding from under the plains. White arrows indicate the boundaries of the plains. 386 m/pixel LORRI image, centered at 52.5°N, 173°E.

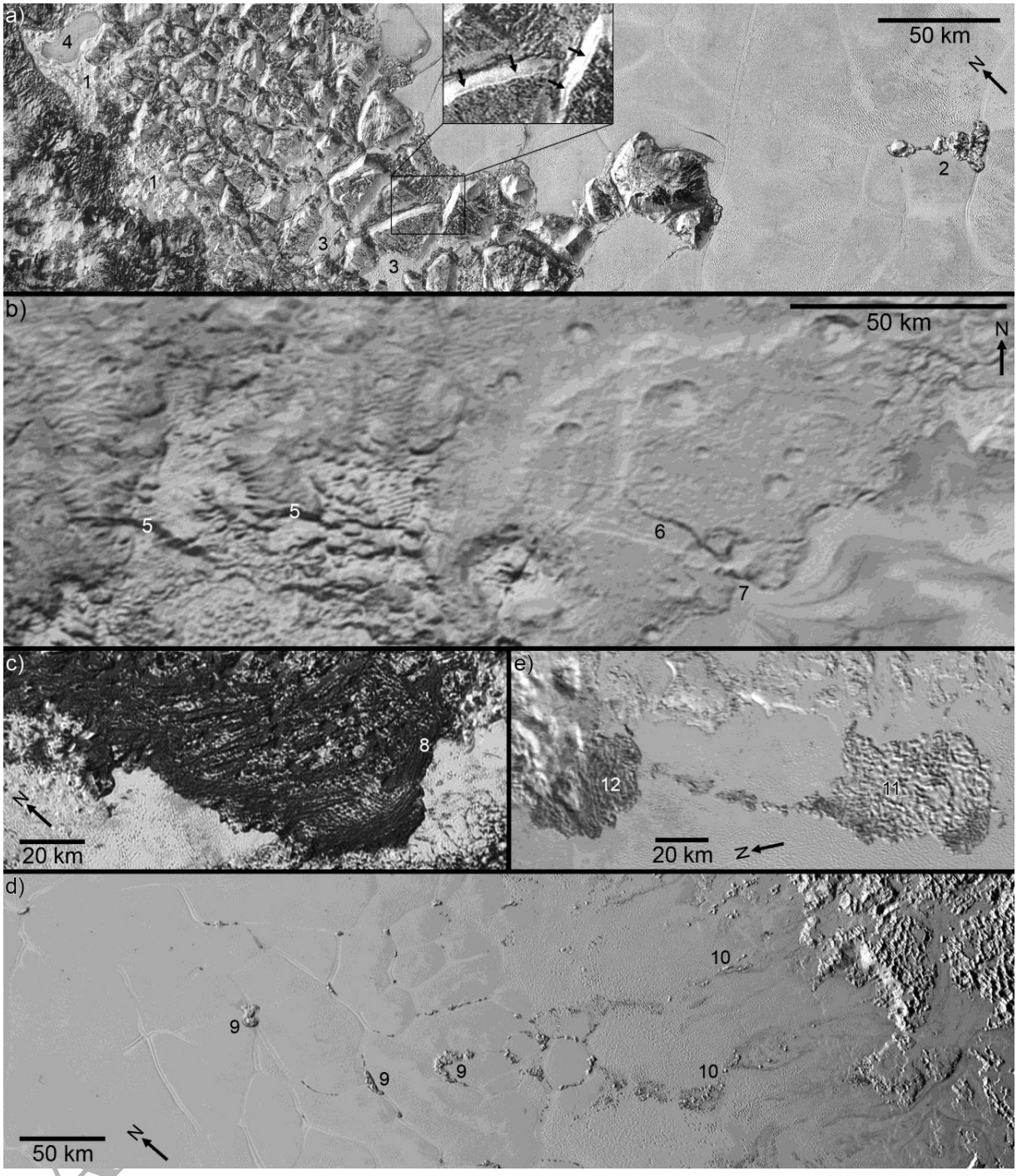

Figure 11. The mountainous and hilly units of Sputnik Planitia. (a) The Chaotic, Angular, Blocky Mountains (unit abm), with a few occurrences of the Chaotic, Inter-Block Material (unit ibm) indicated by '1' labels. '2' label indicates isolated mountains (Coleta de Dados Colles) within Sputnik Planitia's

interior. '3' labels indicate irregularly shaped enclaves of Lightly Pitted Plains that are located interstitially to mountain blocks. '4' label indicates Alcyonia Lacus, an expanse of non-pitted N_2 plains that is surrounded by Chaotic, Angular, Blocky Mountains and Chaotic, Inter-Block Material. Arrows in magnified inset highlight dark layering visible on the faces of mountain blocks. 117 m/pixel LORRI image, centered at 28.5°N, 158°E. (b) Disrupted Pre-Sputnik Planitia Uplands at the northwestern margin of Sputnik Planitia. The Bright, Chaotic Terrain (unit bct) is seen in the western half of the image, and is cut by normal faults ('5' labels). The eastern half of the image features a tilted block of the rough plateau, which is bisected by a graben ('6' label). Dark flow lines in Sputnik Planitia are seen to converge at the point on the shoreline where this graben intersects with the plains ('7' label). 386 m/pixel LORRI image, centered at 46.5°N, 161.5°E. (c) Dark, Ridged Terrain (unit drt). '8' label indicates where ridges appear to curve around to become parallel to the edge of the unit. 234 m/pixel LORRI image, centered at 13°N, 157°E. (d) Scattered Hills (unit sh). View of eastern Sputnik Planitia showing clusters of Scattered Hills ('9' labels) at cell boundaries in the Bright, Cellular Plains. '10' labels indicate chains of Scattered Hills that are coincident with the paths of glacial flow from the Bright, Pitted Uplands. 320 m/pixel MVIC image, centered at 12°N, 188°E. (e) Two large conglomerations of Scattered Hills informally named Challenger Colles ('11' label) and Columbia Colles ('12' label). 320 m/pixel MVIC image, centered at 25.5°N, 196.5°E.

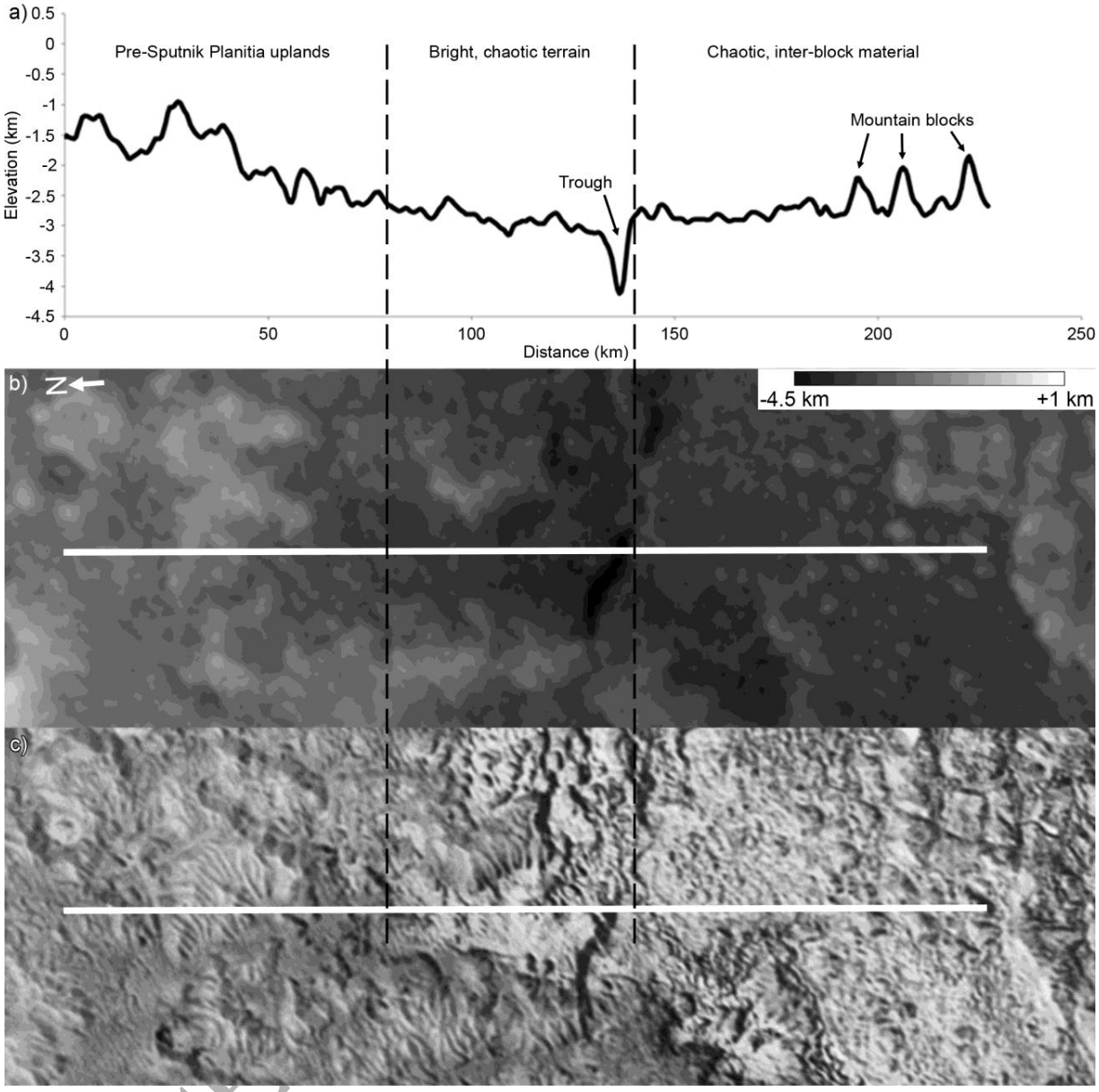

Figure 12. (a) 230 km long topographic profile taken across the northwestern margin of Sputnik Planitia, where the Bright, Chaotic Terrain separates the Pre-Sputnik Planitia Uplands from the Chaotic, Inter-Block Material of Sputnik Planitia itself. The location of the profile on the surface is indicated by white lines in (b), a stereo DEM of the area, and (c), a 386 m/pixel LORRI image (centered at 45.5°N, 156.5°E). Black dashed lines indicate the boundaries of the Pre-Sputnik Planitia Uplands, the Bright, Chaotic Terrain, and the Chaotic, Inter-Block Material on the profile and in the DEM and image. Discounting the

1 km-deep trough and the mountain blocks, the mean level of the Bright, Chaotic Terrain (-2.87 km) is very similar to, and even slightly lower than, the Chaotic, Inter-Block Material (-2.81 km).

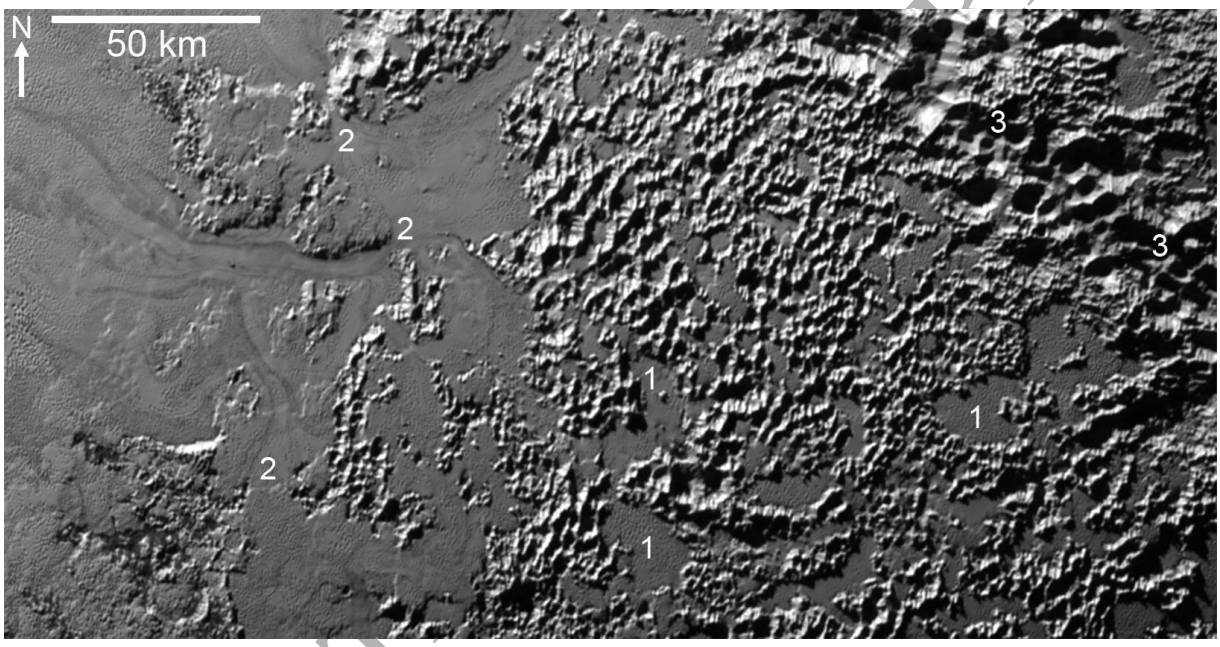

Figure 13. The Bright, Pitted Uplands (unit bpu). '1' labels indicate examples of Patchy, Pitted, Marginal Plains filling wide valleys between pitted terrain. '2' labels indicate the heads of valley glaciers at notches several kilometers wide in the pitted terrain. '3' labels indicate a cluster of large pits, each reaching several kilometers across, which are aligned NW-SE. 320 m/pixel MVIC image, centered at 0.5°N, 198.5°E.

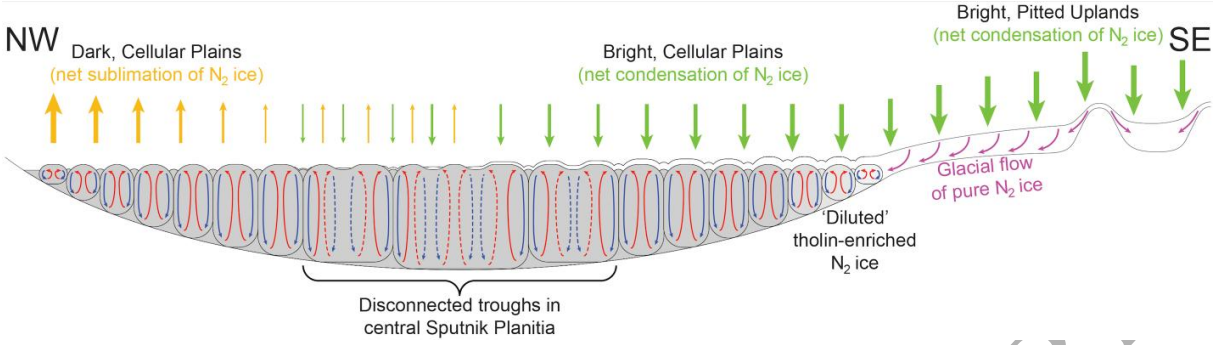

Figure 14. Generalized, vertically exaggerated illustration of a model for how N_2 ice is interpreted to preferentially sublimate from northwestern (NW) Sputnik Planitia and condense on southeastern (SE) Sputnik Planitia and the Bright, Pitted Uplands of eastern Tombaugh Regio. The dark, tholin-enriched N_2 ice of Sputnik Planitia is represented by the gray area. It is this portion of Sputnik Planitia's N_2 ice mass that is undergoing solid-state convection (McKinnon et al., 2016) – the convection is represented by dividing the mass into numerous cells that become wider as Sputnik Planitia's depth increases (assuming an impact basin origin for the topographic low in which the N_2 ice is contained (Schenk et al., 2015; Nimmo et al., 2016)). At the surface, troughs with medial ridges separate the cells. Warm, ascending N_2 ice is represented by red arrows and colder, descending N_2 ice by blue arrows. At the center of Sputnik Planitia, dashed arrows are used to represent the instability of the convection process that is interpreted to cause the disintegration of the trough network in this region – individual cells may be forming and then dissipating, creating surface undulations, but not persisting for long enough to develop an actual trough/ridge morphology at the edges of the cells. The orange and green arrows respectively represent N_2 ice sublimation from and condensation onto the plains, with the weight of the arrow qualitatively representing the magnitude of each process – a thicker arrow represents more intense sublimation/condensation. Purple arrows depict glacial flow back into Sputnik Planitia of N_2 ice that had condensed onto the Bright, Pitted Uplands. The incoming pure N_2 ice may potentially 'dilute' the convecting, tholin-enriched ice along the eastern margin of Sputnik Planitia (although this process cannot be observed as this area is entirely coated with a surficial layer of bright N_2 ice).

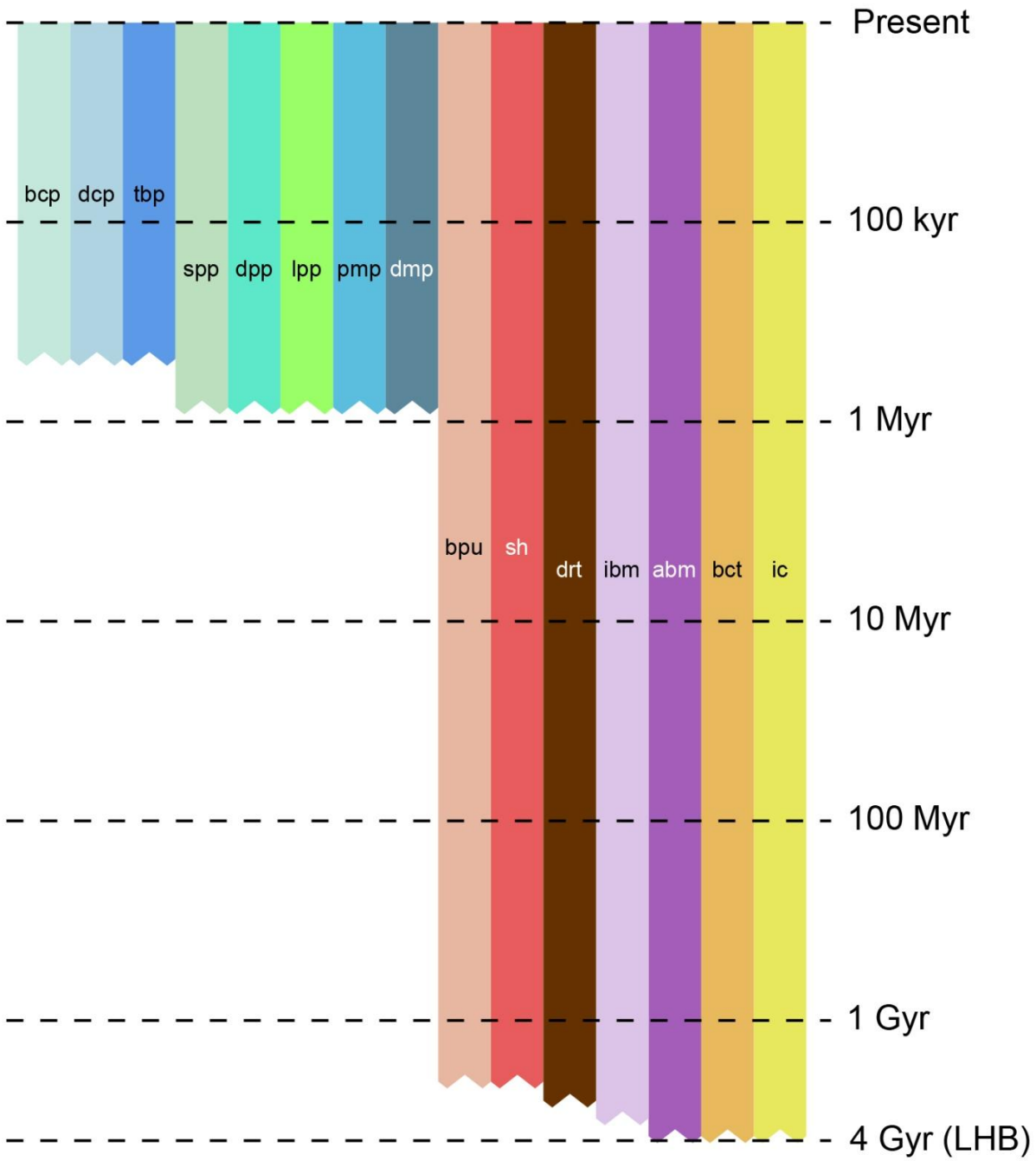

Figure 15. Correlation chart of geologic units mapped in Fig. 5. Stratigraphic positions have been determined by cross-cutting relations, crater size-frequency distributions (in the case of the Bright, Pitted Uplands, unit bpu), as well as considerations of the effect of climate cycles on mobilization of volatiles. Jagged ends of the bars indicate that uncertainties exist in the limits of modification durations.

Table 1. Descriptions and interpretations of units and structural features mapped in Fig. 5, with the exception of the Pre-Sputnik Planitia Uplands.

Unit	Description	Interpretation
Bright, Cellular Plains (bcp)	High albedo plains divided into ovoid cells by a network of troughs, which becomes less interconnected in the center of Sputnik Planitia. Cell interiors typically display a pitted texture at a scale of a few hundred meters towards their edges. No impact craters seen in contiguous 320 m/pixel mapping coverage (like all Sputnik Planitia plains units).	Plains of N_2 ice, recently resurfaced as inferred from the total absence of impact craters. Cellular pattern indicates active solid-state convection occurring throughout the unit. High albedo is caused by condensation of atmospheric N_2 onto the Dark, Cellular Plains to form a thin mantle of pure N_2 ice (also the cause of the high albedo in the non-cellular plains).
Dark, Cellular Plains (dcp)	Similar to the Bright, Cellular Plains, but cell interiors show a lower albedo. Also appears as enclaves within cell centers in the Bright, Cellular Plains, 'filaments' of which are seen to extend into the Dark, Cellular Plains along troughs at the main contact between the two units.	Unit is deficient in N_2 relative to the Bright, Cellular Plains and represents the exposed portion of the convecting N_2 ice mass, which displays a high content of entrained tholins accumulated over the lifetime of Sputnik Planitia.
Dark, Trough-Bounding Plains (tbp)	Very low albedo plains in northern Sputnik Planitia that surround cell margins, which appear as narrow, dark lines. Exhibit flow patterns around obstacles at the margin with surrounding Pre-Sputnik Planitia Uplands.	Occurrence of the plains around dark cell margins may indicate an especially high concentration of entrained tholins in the ice at the edges of the cells and in the bounding troughs. Flow patterns indicate recent mobility of the N_2 ice.
Sparsely Pitted Plains (spp)	Smooth, high albedo plains featuring scattered pits with subdued and softened relief.	Deeply or Lightly Pitted Plains that have been resurfaced by relaxation/infilling of pit topography by flow of N_2 ice, and/or blanketing by atmospheric N_2 condensing on the surface.

Deeply Pitted Plains (dpp)	High albedo plains featuring dense concentrations of sharply defined pits that reach a few km across. Pits can be single or merge to form doublets and aligned chains of joined pits. Pit swarms sometimes form wavelike patterns. Elongate pits tend to align N-S in southern Sputnik Planitia. When pit floors can be resolved, they always display a low albedo.	Pits form via sublimation that may be widening existing fractures formed by ice shearing in the N_2 ice plains. Low albedo floors may be dark substrate of Sputnik Planitia, or tholins entrained in the ice that have been liberated by sublimation and built up as a lag. Wavelike patterns may reveal structural anisotropies in the ice (i.e. stress fields associated with flow paths).
Lightly Pitted Plains (lpp)	High albedo plains displaying a shallow, densely pitted texture at a scale of a few hundred meters.	Continuous, shallow pitting represents sublimation of N_2 ice across the whole surface, rather than at discrete, possibly structurally controlled locations like in the Deeply Pitted Plains.
Patchy, Pitted, Marginal Plains (pmp)	High albedo, often-hummocky plains on the margins of Sputnik Planitia and in basins and valleys of the Bright, Pitted Uplands. Generally displays a patchy texture of close-spaced shallow pits interspersed with smooth, featureless zones. Dark flow lines are often seen where the unit occurs in valleys leading from the Bright, Pitted Uplands to Sputnik Planitia.	Shallow N_2 ice draped over underlying topography, which may contribute to the heterogeneous texture of the unit. Glacial flow of the unit is occurring from valleys in the Bright, Pitted Uplands to the open plains of Sputnik Planitia.
Dark-Pitted, Marginal Plains (dmp)	High albedo plains displaying chains of elongate, dark-floored pits interspersed with smooth, lightly pitted zones. Unit occurs on the western edge of Sputnik Planitia, and on the floors of some craters in Cthulhu Regio.	Shallow N_2 ice draped over underlying topography. The ice may be residual and relatively immobile compared to that of the Patchy, Pitted, Marginal Plains. Dark floors of the pits are likely to be the dark terrain of Cthulhu Regio, which this unit overlies.

Chaotic, Angular, Blocky Mountains (abm)	Discontinuous chain of mountain ranges, consisting of angular blocks with random orientations, reaching up to 40 km across and 5 km high. Ranges extend along the western margin of Sputnik Planitia, with a few isolated blocks occurring within its interior.	Fragments of the H_2O ice crust that have been disrupted by tectonism and intruded by N_2 ice of Sputnik Planitia, and which are now grounded and tilted within shallow N_2 ice. Smaller blocks within Sputnik Planitia's interior may be floating in deeper N_2 ice.
Chaotic, Inter-Block Material (ibm)	Chaotically oriented, close-packed blocks, reaching several km across, that are interstitial to and embay the Chaotic, Angular, Blocky Mountains.	Similar genesis to the Chaotic, Angular, Blocky Mountains, but finer texture may indicate breaking up of mountain blocks into smaller fragments and/or size filtering thereafter if the blocks are mobile in the N_2 ice.
Scattered Hills (sh)	Hills scattered across east Sputnik Planitia that reach a few km across. Tend to collect into densely packed clusters reaching tens of km across. Proximal to the Bright, Pitted Uplands, chains of hills align along paths of glacial flow. In the Bright, Cellular Plains, they are always coincident with the cell boundaries.	H_2O or CH_4 ice fragments eroded from the Bright, Pitted Uplands material that have rafted into Sputnik Planitia on valley glaciers of less dense N_2 ice. In the Bright, Cellular Plains, convective motions corral them into clusters at cell boundaries.
Dark, Ridged Terrain (drt)	Situated between the Chaotic, Angular, Blocky Mountains of western Sputnik Planitia and the Pre-Sputnik Planitia Uplands. Aligned ridges are oriented parallel to the edge of Sputnik Planitia, and display wavelengths from several hundred meters to a few km.	Possibly Chaotic, Inter-Block Material covered by dark mantling material. Compression of this unit by pressure exerted from westward motion of the Chaotic, Angular, Blocky Mountains may produce the ridges.
Bright, Pitted Uplands (bpu)	High albedo, rugged terrain displaying a pervasive pitted texture, with individual pits reaching several km across. The pits can locally intersect to form distinct NE-SW-trending ridge-	Pitted texture may form through a combination of sublimation and undermining/collapse of a CH_4 ice deposit. High albedo caused by condensation of N_2 ice as a thin mantle covering the surface.

	and-trough terrain. NW-SE-trending troughs composed of especially large pits (<10 km across and <1 km deep) are also seen. Spatial density of impact craters is low.	Flow downslope of N_2 ice causes it to collect in basins, where it forms Patchy, Pitted, Marginal Plains. Large troughs are structurally controlled and indicate surface collapse above extensional fault lines.
Bright, Chaotic Terrain (bct)	High albedo plains interspersed with darker blocks reaching several km across, on the northwest margin of Sputnik Planitia. E-W oriented troughs and scarps cross the unit. Parts of the unit are depressed by several hundred meters below the bordering Chaotic Inter-Block Material.	Unit represents material of the Pre-Sputnik Planitia Uplands that is experiencing extensional tectonism and subsidence, and possible intrusion by N_2 ice of Sputnik Planitia. High albedo of the plains indicates a surface covering of N_2 ice, possibly 'overflowed' from Sputnik Planitia. Unit may represent an incipient stage of formation of the Chaotic, Angular, Blocky Mountains.
Impact Crater (ic)	Impact craters >2 km in diameter that show complete rims and fresh to moderately degraded morphologies. Mostly occur in the Pre-Sputnik Planitia Uplands to the west and north of Sputnik Planitia.	Craters formed by impacts into Pluto's surface.
Graben	Linear troughs that can reach up to 1 km in depth and more than 200 km in length. Oriented NE-SW or E-W. Occur within the Pre-Sputnik Planitia Uplands, Bright, Pitted Uplands, and Bright, Chaotic Terrain.	Extensional tectonic features comprising parallel normal faults bounding a depressed block. Parallel alignment of graben and scarps indicates regional-scale crustal extension.
Scarp	Linear cliffs that can reach up to several hundred meters high and over 100 km in length. Oriented NE-SW or E-W. Occur within the Pre-Sputnik Planitia Uplands, and Bright, Pitted Uplands.	Extensional tectonic features comprising a normal fault with downthrown and upthrown blocks on either side. Parallel alignment of graben and scarps indicates

		regional-scale crustal extension.
Trough in cellular plains	Network of troughs dividing the N_2 ice plains of Sputnik Planitia into discrete cells. Some troughs are isolated within cells. Troughs reach a few km across and tend to exhibit medial ridges, especially in the Bright, Cellular Plains. Troughs appear as dark lineations ~1 km across in the Dark, Trough-Bounding Plains, with medial ridges occasionally apparent. Trough depths estimated at several tens of meters.	Trough/ridge morphology formed at the convergence of laterally migrating N_2 ice at cell boundaries, due to solid-state convection of the N_2 ice here. Trough relief may be less apparent in the Dark, Trough-Bounding Plains due to tholins filling the troughs.
'Extinct' trough	Occur to the south of the Bright, Cellular Plains. Chains of elongated, dark-floored pits tracing the outlines of elongate, vaguely triangular polygons, with Sparsely Pitted Plains existing within their centers.	Former cells that experienced convection within the N_2 ice plains, but with southward motion of the ice having shifted them away from the convective zone, causing the relief of their interiors and bounding troughs to relax. Tholin deposits that filled the troughs still mark the outlines of former cells on the floors of pits of the Deeply Pitted Plains unit.
Valley glacier flow line	Dark, often sinuous lineations that extend from valley floors bordering the eastern edge of Sputnik Planitia to plains several tens of km within its interior. Lineations reach a few km across that reach up to ~100 km long, and are not very apparent at low phase angle.	Lineations represent blocky material eroded from the surrounding Bright, Pitted Uplands that has been deposited on flowing N_2 ice valley glaciers, and which is forming rubbly lateral moraines along the margins of the glaciers.